Calcium and strontium isotope constraints on water mixing, carbonate fluxes and fish migration in Coorong Lagoon, South Australia

Thesis submitted in accordance with the requirements of the University of Adelaide for an Honours Degree in Geology

Yuexiao Shao

November 2016

THE UNIVERSITY of ADELAIDE

CALCIUM AND STRONTIUM ISOTOPE CONSTRAINTS ON WATER MIXING, CARBONATE FLUXES AND FISH MIGRATION IN COORONG LAGOON, SOUTH AUSTRALIA

CA AND SR ISOTOPES IN COORONG-MURRAY MOUTH

ABSTRACT

To better understand the water chemistry and sources of water inputs to Coorong Lagoon, the terminal estuary of Australia's largest river system (i.e. Murray), we established water mixing models using Sr and Ca isotopes (i.e. measuring $^{87}Sr/^{86}Sr$ and $\delta^{44/40}Ca$ signatures) and investigated the sensitivity of these isotope proxies to salinity changes along the lagoon (ranging from fresh to hypersaline, i.e., 0 to ~120 PSU). Additionally, fish otoliths of the smallmouth hardyhead (*Atherinosoma microstoma*) are used as an intergrated average values of local water signatures over one-year (i.e. the fish's lifespan). Basically, the lagoon waters were considered as a result of brackish/fresh water – seawater mixing, with the strong effect of evaporation, which caused hypersalinity in the south part of the lagoon. From the water mixing models, the North Lagoon is strongly controlled by seawater input from Southern Ocean except when temporary groundwater input events occured; the South Lagoon is mostly hypersaline, as a result of seawater – groundwater mixing and evaporation, and inputs from both components were significant, confirmed by Sr isotope signatures in waters and otoliths. The effect of water evaporation, which leads to oversaturation of carbonate minerals (i.e., calcite and aragonite) in lagoon waters, has also an impact on the Ca isotope composition of local waters, as these yielded systematically heavy $\delta^{44/40}Ca$ signatures due to removal of light Ca isotopes into $CaCO_3$. Our modelling of Ca isotope data suggests that about 35 - 40% of Ca in the South Lagoon waters has been removed as CaCO3, which in has

implications for understanding of a local carbon cycling in the lagoon. Finally, results of this study also provide basis for future applications of Sr and Ca isotopes that aim to reconstruct ancient environmental conditions and paleo-salinity changes in the Coorong lagoon based on sediment core record and/or fossil archives.

KEYWORDS

Strontium, Calcium, Isotope, Coorong, Salinity, Water mixing, Otoliths

TABLE OF CONTENTS

LIST OF FIGURES AND TABLES

1. INTRODUCTION

The Coorong Lagoon, together with the Lower Lakes (Lake Alexandrina and Lake Albert), form the terminus of Australia's largest river system (i.e. Murray) at its mouth to the Southern Ocean in South Australia. It is a string of saltwater lagoon approximately 140 km in length, sheltered from the Southern Ocean by a line of barriers (i.e. the Holocene sand dunes) (Kjerfve, 1986; Knoppers, 1994). The lagoon is divided into North and South Lagoons, with a narrow connection called Parnka Point between the two.

The water of the Coorong Lagoon exchanges with the Southern Ocean waters through Murray Mouth, which is a relatively narrow channel towards the northern end of the lagoon; where major fresh water input from the River Murray and Lake Alexandrina used to occur until a line of barrages were constructed between 1935 and 1940, which isolated Lake Alexandrina from the saline waters of the Coorong (Webster, 2010). Due to its limited access to the ocean and highly reduced input of freshwater, the South Lagoon has become hypersaline over the last five decades (Webster, 2010).

With such a unique lagoon-estuary hydrological and ecological system and salinity ranging from fresh through brackish to hypersaline, the Coorong represents a natural laboratory for calibrating traditional and novel isotope proxies (e.g., Sr and Ca isotopes) with respect to salinity changes and water mixing phenomena in marine coastal systems. Strontium (Sr), as a sensitive geochemical tracer, has been widely used in large-scale ecosystem and hydrological studies, in particular as $^{87}Sr/^{86}Sr$ ratios of water samples reflect the sources of Sr available during their formation (e.g. oceanic water vs. continental water). Moreover, with the distinctive $^{87}Sr/^{86}Sr$ ratios of water sources, the relative proportions of these sources in the lagoon can be determined (Capo et al., 1998).

As a radiogenic isotope tracer, $^{87}Sr/^{86}Sr$ in biominerals can also reflect past changes in ambient environments or reconstruct organisms' environmental life histories.

Therefore, combining both water and biomineral Sr and Ca isotope data can provide key information about present and past hydrological and environmental histories of the Coorong Lagoon and the species within it.

Based on that, the present project had two major components, which are (i) to better understand the natural variability of Sr and Ca isotope compositions in waters from the Coorong region and their sensitivity to salinity changes and water-mixing processes; and (ii) to test Sr and Ca isotopes as proxies in bio-minerals (i.e., otoliths) of a selected fish species (*Atherinosoma microstoma*) with relatively low mobility to infer past changes in the lagoon hydrology and to investigate fish movement patterns. On one hand, we aimed to understand the water chemistry of the lagoon, including a) the salinity profile, b) concentrations of major and trace elements and their relationships with salinity, and most importantly, c) isotope compositions ($^{87}Sr/^{86}Sr$ and $\delta^{44/40}Ca$) as indicators of input sources. On the other hand, we aimed to investigate past movements of fish (i.e., over ca. 1 year period the life span of the studied fish species), using isotopes in a biomineral called fish otolith (i.e. ear-stones composed of aragonite). Previous studies by Gillanders and Munro (2012), Kraus and Secor (2004) and Brown and Severin (2009) have indicated that the utilisation of elemental Sr/Ca ratios may have a few constraints, particularly in hypersaline coastal settings, likely due to physiological regulation and species-specific biological processes on elemental incorporation and Sr/Ca ratios in otoliths. Therefore, this study aims to use for the first time the isotope systems of Sr and Ca as a multi-proxy isotope approach – to further investigate if the limitations and issues associated with elemental Sr and Ca proxies in otoliths might be resolved with Sr and Ca isotope studies.

Thus, our analyses include (i) the coupled isotope measurements of $^{87}Sr/^{86}Sr$ and $\delta^{44/40}Ca$ values in fish otoliths and local lagoon waters, as well as (ii) analysis in single otoliths with higher spatial and temporal resolution throughout a fish's entire lifespan.

Ultimately, this study utilised Sr and Ca isotopes to better understand the hydrology, water mixing and fish migration in a modern coastal environment (i.e., the Coorong region), which will have implications for future studies aiming at palaeo-salinity and paleo-migration reconstructions via the applications of ancient biocarbonates and alkaline earth metal (Ca, Sr, Mg and Ba) isotope systems.

2. BACKGROUND

2.1. Water mixing regime in the Coorong region

The Lower Lakes and Coorong region (Fig. 1), are strongly under the effects of the saltwater wedge intruding from the Southern Ocean, from fresh terrestrial water or groundwater located above seawater, and a zone of mixing, where seawater and groundwater interact (Haese et al., 2008).

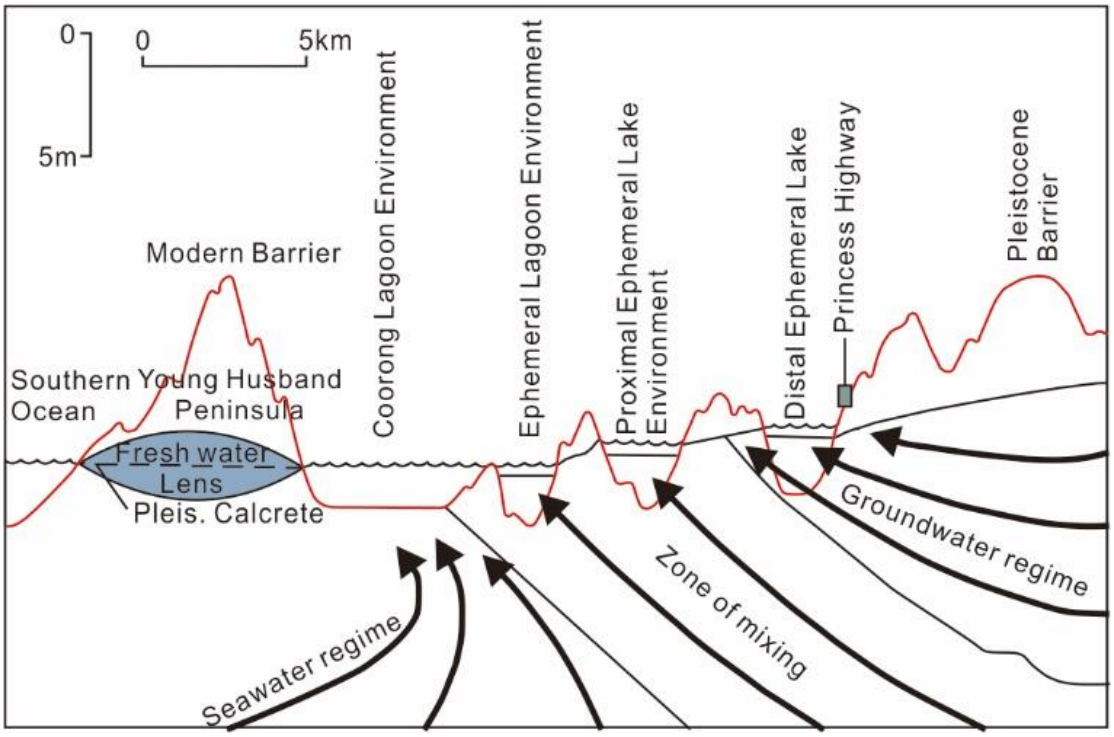

Figure 1: Generalised cross section of Coorong Lagoon and the coastal area which form a mixing zone of seawater and groundwater regimes (from von der Borch, 1975).

2.1.1. SALINE WATER INPUT

The major saline water input to the Coorong Lagoon is from the Southern Ocean water via the Murray Mouth by tidal waves, which occurs close to the northern end of the lagoon. Only after 2002, has Murray Mouth been maintained constantly open via a dredging program (Webster, 2010). Before that, the mouth varied from hundreds of metres wide to entirely closed in 1981 (Walker, 2003; Webster, 2010).

2.1.2. FRESHWATER INPUTS/OUTPUTS

2.1.2.1. Barrage flows

Barrage flows from Lake Alexandrina enter the Coorong Lagoon during times of high discharge from the River Murray. Due to the positions of the barrages, barrage flows only flush between the barrages and Southern Ocean, and their influence on water chemistry is mostly limited to the north lagoon and the Murray Mouth (Webster, 2010).

2.1.2.2. Groundwater

Groundwater input has been observed in different locations along the lagoon, mostly short-lived. According to Noye (1975), groundwater was found on the western side of Coorong, i.e. the Younghusband Peninsula sand barrier (Haese et al., 2009). Haese et al. (2009) also observed and described active seeps on the east side of the lagoon, which were considered sourced from an unconfined aquifer draining sea-wards (cf., von der Borch, Lock, and Schwebel (1975).

2.1.2.3. Evaporation

Evaporation is the major pathway for water output in the lagoon system, and its importance is supported by oxygen isotope ($\delta^{18}O$) in the lagoon waters (Kell-Duivestein, 2015), where the southern lagoon with highest salinities also yielded the heaviest $\delta^{18}O$ values (Gillanders & Munro, 2012).

2.2. Salinity and water chemistry

Generally, the salinity of the North Lagoon is marine-like (i.e., ~35 PSU) due to frequent exchange with the Southern Ocean. A sudden transition in salinity occurs near Parnka Point where waters become hypersaline (>70 PSU), which is a common feature for the entire South Lagoon. Following the construction of the barrages between Pelican Point and Goolwa, the salinity of the South Lagoon has been increasing for decades, except for the early 1970s, when the barrage flows were strong. Due to the decline of barrage flows, the South Lagoon waters reached salinities that are ca. four times higher (i.e., in excess of 120 PSU) compared to the Southern Ocean (Fernandes & Tanner, 2009).

In 2012, the salinity of South Lagoon was ~120 PSU (Gillanders & Munro, 2012) and went up to 140 in 2015 (Kell-Duivestein, 2015). Gillanders and Munro (2012)

investigated the effect of hypersaline conditions on water chemistry of the Coorong and the elemental patterns in fish otoliths. Specifically, they studied concentrations of Ba, Sr, Mn, Mg and Ca in water samples; the results indicate a strong positive correlation between Mg concentration and salinity. Sr and Ca concentrations in waters also showed the same correlation with salinity, though with greater variation was found at higher salinities, possibly reflecting precipitation of aragonite from water, which begins when the lagoon water reaches twice the concentration of seawater. Finally, Ba concentrations in waters showed a more complex relationship with salinity, whereby Ba declined from freshwater through to marine waters, but then increased with increasing salinity, a trend not observed for other elements.

2.3. Otoliths chemistry

The elemental and stable isotope compositions of otoliths from smallmouth hardyheads (*Atherinosoma microstoma*) collected in Coorong lagoons, conducted by Gillanders and Munro (2012), focused on multiple proxies, including: Ba/Ca, Sr/Ca, Mg/Ca, Mn/Ca, Na/Ca, Li/Ca, $\delta^{18}O$ and $\delta^{13}C$. These were then compared to the same proxies measured in local waters with a range of salinities, but generally no robust correlation patterns were found between these elemental proxies in waters and otoliths collected from the same location (Gillanders & Munro, 2012).

Specifically, the Sr/Ca ratio in otoliths remains relatively constant at around 3.5mmol/mol with respect to changing salinities in lagoon water. This ratio has been widely applied as a tracer of fish movement between freshwater and marine habitats, with the assumption that low salinity habitats correspond to lower Sr/Ca in otoliths, and generally negative correlation patterns were observed between Sr/Ca and salinity across a range of brackish estuarine systems (Kraus & Secor, 2004). This trend however was not

observed in hypersaline coastal settings, which in turn makes the application of the otolith Sr/Ca proxy problematic in high salinity regimes (Kraus & Secor, 2004). Brown and Severin (2009) also suggested that water Sr/Ca composition is the primary factor influencing the otolith Sr/Ca for freshwater fish species, but not marine species. Thus, overall the utilisation of Sr/Ca ratios in otoliths is challenging in marine, and particularly hypersaline settings.

There are several possible explanations for this decoupling of Sr/Ca in otoliths and waters. Firstly, since Ca^{2+} ions in $CaCO_3$ mineralogy of otoliths can be substituted by other trace elements with similar ionic radius and charge (such as Sr^{2+}), the incorporation of Sr into otoliths can be strongly controlled by biomineralisation processes (Elsdon & Gillanders, 2003). This leads to different relationships between water and otoliths element-to-Ca ratios depending on different substituting elements and specific conditions of the fish otolith biomineralisation. Thus, the microchemistry of the local calcifying fluids in fish will also influence the otolith Sr/Ca composition (Milton & Chenery, 2001), being strongly biologically controlled and species-specific.

As a result, a variety of effects of salinity on fish otolith Sr/Ca ratios have been reported in literature, which can be either positive or negative, or even with no systematic relationship (Chesney et al., 1998; Dorval et al., 2007; Elsdon & Gillanders, 2002, 2004; Fowler et al., 1995; Hoff & Fuiman, 1995; Martin & Thorrold, 2005; Martin et al., 2004).

2.4. Strontium and Calcium isotope systematics

2.4.1. STRONTIUM ISOTOPES

Due to the above issues associated with the biological control of elemental Sr/Ca proxy in fish otoliths, we focused our study on isotope composition of strontium, i.e., $^{87}Sr/^{86}Sr$

ratio, to determine water sources and fish migration in the Coorong lagoon. Strontium (Sr) has four stable and naturally occurring isotopes, which are ^{84}Sr, ^{86}Sr, ^{87}Sr and ^{88}Sr. ^{87}Sr is a radiogenic isotope generated by emission of a negative β-particle from ^{87}Rb, which has a half-life of 4.99×10^{10} years. As an incompatible element, Rb was excluded from mantle melts and incorporated into continental crust by the process of fractional crystallisation during early differentiation of crust and mantle. As a result, continental crust has higher Rb concentration than the upper mantle, as ^{87}Rb decays overtime, continental rocks yield higher $^{87}Sr/^{86}Sr$ ratios than the mantle and mantle derived basaltic rocks. These $^{87}Sr/^{86}Sr$ signatures in different rock types are further reflected in different water sources, where continental-sourced waters typically have more radiogenic $^{87}Sr/^{86}Sr$ signatures than ocean-sourced waters (i.e. seawater).

Unlike elemental Sr/Ca ratios, the radiogenic $^{87}Sr/^{86}Sr$ proxy is not sensitive to biological proxesses, and strictly reflects the sources of Sr in local waters available to fish during the otolith formation. Thus, the $^{87}Sr/^{86}Sr$ proxy is considered as a powerful geochemical tracer of distinct water masses and/or Sr sources in the earth surface and coastal environments (Capo et al., 1998), where different Sr sources mix (e.g. continental rivers, groundwaters vs. seawater).

2.4.2. CALCIUM ISOTOPES

Calcium (Ca) has six stable isotopes: ^{40}Ca, ^{42}Ca, ^{43}Ca, ^{44}Ca, ^{46}Ca and ^{48}Ca, where $^{40}Ca/^{44}Ca$ ratio (or $\delta^{44/40}Ca$ value) is commonly used to express the natural variability of Ca isotope signature in samples and is broadly applied in environmental and biological studies to elucidate the bio-geochemistry of global Ca cycle. Compared to the radiogenic $^{87}Sr/^{86}Sr$, the stable Ca isotope proxy ($\delta^{44/40}Ca$) is also sensitive to biological processes (i.e., mass-dependent fractionation effects), and requires measuring through use of a Ca

double spike (Fantle & Tipper, 2014). For normalisation, $\delta^{44/40}$Ca of a sample is normalised to modern seawater, or SRM 915a standard, so the delta Ca isotope notation is expressed as:

$$\delta^{44/40}\text{Ca (or } \delta^{44}\text{Ca)} = \left(\frac{(^{44}\text{Ca}/^{40}\text{Ca})_{sample}}{(^{44}\text{Ca}/^{40}\text{Ca})_{seawater}} - 1\right) \cdot 10^3 \quad \text{(Eq. 1)}$$

According to Fantle and Tipper (2014), the overall range of $\delta^{44/40}$Ca in nature is about 4‰, ranging from about -2 to +2‰, based on the compilation of 73 studies and over 2600 data points. This natural variability of δ^{44}Ca on Earth is shown in Fig. 2, where the data are normalised to SRM 915a (instead of standard seawater), where $\delta^{44/40}$Ca of modern seawater is close to +1.9 ‰. Note that in our study all measured and presented $\delta^{44/40}$Ca data are normalised relative to modern seawater (i.e., $\delta^{44/40}$Ca of seawater = 0 ‰).

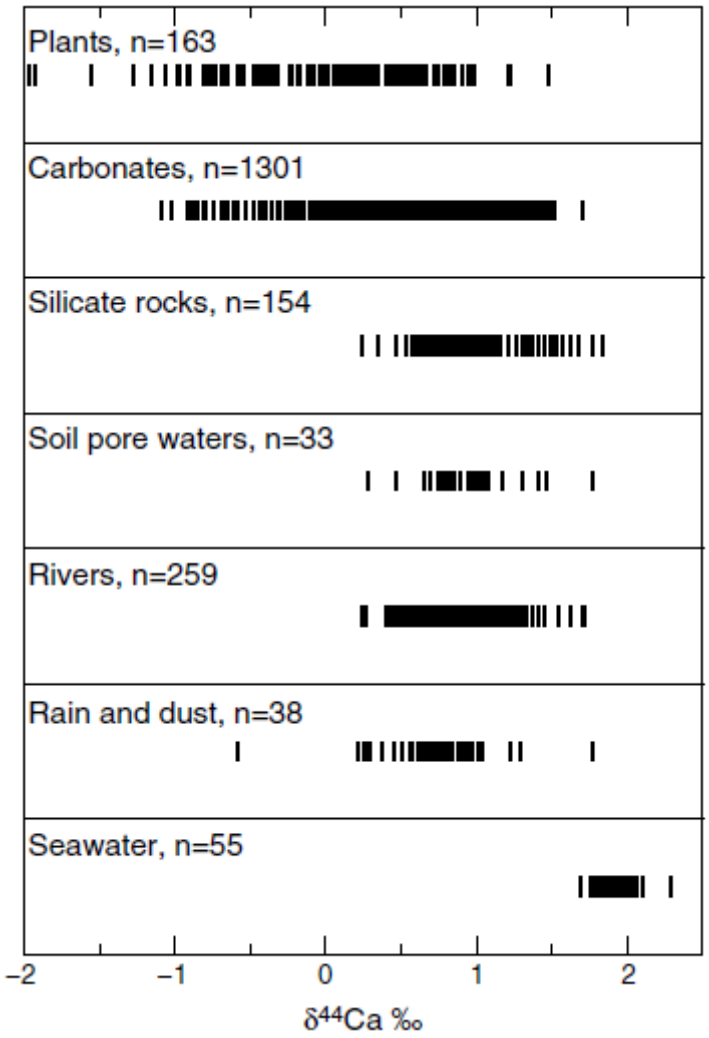

Figure 2: Summary of the Ca isotope data ($\delta^{44}Ca$ or $\delta^{44/40}Ca$ relative to SRM-915a, ‰) (Fantle & Tipper, 2014).

3. METHODS

3.1. Study sites and samples

Samples of water and otoliths used in this study were collected from the Coorong Lagoons and Murray Mouth (see Fig. 3). In total we collected 41 new samples this year, including 13 water samples, 24 fish in the Coorong and 4 South Australian rainwater samples; there were also 31 water samples from 2015 analysed or used in this study, which were collected by Kell-Duivestein (2015) from the inlet of River Murray (Wellington), the Lower Lakes, the Coorong Lagoon as well as the reference seawater

collected from the Southern Ocean. Detailed coordinates and sampling dates for our sampling sites are listed in the Appendix C (Table C1).

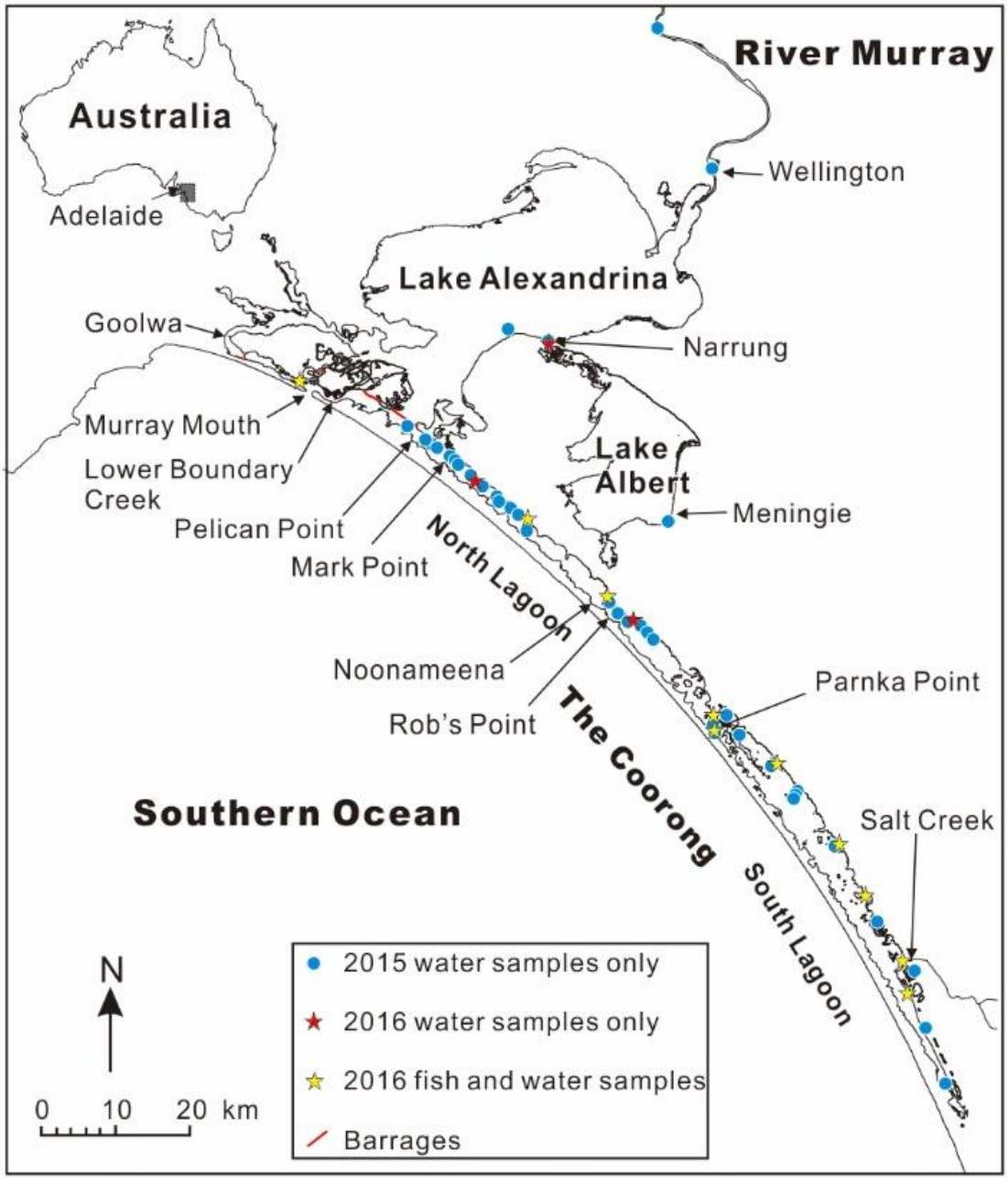

Figure 3: A map of Lower Lakes and Coorong Lagoon at the terminal end of Murray River, South Australia. Sampling locations of study are highlighted and distinguished between years; key levers of Coorong hydrodynamics are shown. Red bars in North Lagoon between Pelican Point and Goolwa show barrage locations. Dot points stars of different colours represent sampling sites.

3.1.1. WATER SAMPLES

Water samples were collected from the surface of the water bodies, which have been well mixed by wind; water temperature, pH, and salinity/total dissolved solids (TDS) were measured in situ by HI-98194 Multiparameter at the same time the sample was collected, and GPS coordinates of each sample site were also recorded (Kell-Duivestein, 2015). Sampling of water was done in April and May 2015 by Kell-Duivestein (2015) and in May 2016 (this study). In May 2015, two additional groundwater samples were taken from two separate wells located ca. 800 m apart near Noonameena (Kell-Duivestein, 2015).

3.1.2. FISH SAMPLES

The fish species collected in the Coorong lagoons for this study were the smallmouth hardyheads (*Atherinosoma microstoma*) which has a total length of less than 110 mm and an annual life cycle (Gillanders & Munro, 2012; Wedderburn et al., 2014). This species lives usually within ca. 2 m of water depth amd feeds on small invertebrates and plankton. Due to the extreme salinity tolerance of the study species (i.e., from 3.3 to 108 PSU; (Lui, 1969)), the hardyheads were caught and sampled across the entire Coorong lagoon system as well as the Murray mouth estuary.

3.1.3. LOCAL SOUTH AUSTRALIAN RAINWATER SAMPLES

Four rainwater samples were collected about 100 km north from the North Coorong Lagoon (and about 200 km from the Southern Lagoon) to further constrain the isotope composition of local atmospheric deposition, and its possible impact on water mixing and isotope signatures observed in the Coorong lagoon system. Samples of Rain-IT and Rain-PT, were collected from a galvanised iron tank and a polyethylene tank, respectively,

representing a long-term local rain water source that was accumulated and sampled into the tanks over a period of several years. In addition, samples Rain-A and Rain-B were collected by two 2 L acid cleaned polypropylene bottles on 29th and 30th August 2016, thus representing a short-term and recent rain events. For each sample, about 200 mL of rainwater was collected.

3.2. Sample preparation – Waters and Otoliths

All materials for water sampling were washed in 10% HNO_3 and dried before use, and teflonwares for isotope and elemental analysis were cleaned in 6M HNO_3 at 170 °C on a hotplate for 48 hours, rinsed with DI (i.e., deionised) water and further cleaned in 6M HCl at 170 °C for 24 hours and dried.

Water samples were filtered with 0.45 µm Whatman® Cellulose Nitrate Membrane Filters to remove insoluble particles before elemental and isotopic analyses, and filtered waters were stored in acid-cleaned 15 mL polypropylene test tubes.

For the fish samples, 2-3 biggest fish were selected from each sampling site, total length (TL) of each fish was measured (in mm), and their wet weights were also measured (g) using a two decimal places balance. Sagital otoliths were removed from each fish's head under a dissecting microscope, cleaned of adhering tissue in milliQ water, and transferred to a 1.5 mL centrifuge tube and stored dry. The otoliths were weighed using a six decimal places precise balance and recorded in mg.

In order to get a more detail picture of temporal $^{87}Sr/^{86}Sr$ variation at different stages of the fish's life, the largest otoliths, one from North Lagoon (sample C03-03) and one from South Lagoon (sample C10-03), were chosen for micro-drilling and subsequent isotope analysis.

3.3. Elemental concentration analyses

Elemental concentrations of filtered water samples (i.e., Ca, Sr, Mg, Ba, Mn, Fe, Na, Zn, Cu) were measured with an Agilent 7500cs solution ICP-MS at Adelaide Microscopy in Adelaide, Australia. As the detection range of solution ICP-MS is 10-10,000 ppb for most elements, to ensure concentrations of all measured elements were within this interval, water samples were diluted with 5% HNO3 into two series: a) 10x dilution factor, for detecting Sr and trace elements, and b) 100x dilution factor, for detecting highly concentrated elements (i.e. Na, Ca and Mg). Diluted solutions of samples were loaded in 5 ml vials for solution ICP-MS analysis. Typical analytical error was on the order of ca. 3%. The measurement results can be seen in Table C4, Appendix C, and plots of concentrations against salinity are in Fig. C1, Appendix C.

3.4. Strontium isotope analyses ($^{87}Sr/^{86}Sr$ ratios)

3.4.1. CHROMATOGRAPHIC PURIFICATION

The first step of measuring isotope compositions $^{87}Sr/^{86}Sr$ was to separate the Sr from the sample matrix, and this was accomplished using prepFAST-MC with Hepa filtered air supply, controlled by ESI software from the computer. Note that the prepFAST-MC system was installed in January 2016, so all calibrations and tests for elemental purifications were accomplished as a part of this study, following the procedures described in Romaniello et al. (2015). See Appendix A.1 for detailed procedures.

3.4.2. TIMS ANALYSES – STRONTRIUM

High precision measurements of $^{87}Sr/^{86}Sr$ in water samples and otoliths were done by the thermal ionisation mass spectrometry (TIMS), i.e., Phoenix TIMS instrument, with a reproducibility at two standard errors (2se) better than 0.000005, as determined by repeat measurements of standards and/or multiple replicates of individual samples. The Sr standard used for our TIMS measurements was SRM 987. Detailed protocols of sample loading and filament ionasation, and reproducibilities of the measured $^{87}Sr/^{86}Sr$ ratios are shown in Appendix A.2 and A.3.

3.5. Calcium isotope analyses ($\delta^{44/40}Ca$)

3.5.1. CHROMATOGRAPHIC PURIFICATION AND TIMS MEASUREMENTS

To determine the Ca isotope composition (i.e., $\delta^{44/40}Ca$) of our samples, we used a "double spike" approach (i.e. ^{43}Ca–^{42}Ca isotope tracer), based on the methods described in Holmden and Bélanger (2010) and Farkaš et al. (2016). Prior to the Ca isotope analysis all samples were passed through the cation exchange resin (Holmden & Bélanger, 2010), and the subsequent isotope analysis of purified Ca fractions from selected waters and otoliths were performed using Thermo Triton TIMS instrument at the Saskatchewan Isotope Laboratory (Canada), with a typical 2SE reproducibility on $\delta^{44/40}Ca$ value of about 0.05 per mil, or better (for details see Table 1).

4. OBSERVATIONS AND RESULTS

Here we present results of this study which include water temperature, salinity and isotope composition (i.e. $^{87}Sr/^{86}Sr$ and $\delta^{44/40}Ca$) in collected waters and otoliths (see Table 1-3). Results are also plotted as a function of latitude in Fig. 4.

Table 1. $^{87}Sr/^{86}Sr$ and $\delta^{44/40}Ca$ data (with temperatures and salinities) for water samples, and for bulk otoliths. For detailed sampling locations and dates, see Table C1 in Appendix C.

Sample ID	Area	Water temperature (℃)	Salinity (PSU)	$^{87}Sr/^{86}Sr$ ± 2se	$\delta^{44/40}Ca$ ± 2se
Coorong Lagoon water samples					
M13	Murray Mouth	18.00	35.00	0.709180 ± 0.000003	
C02	North Lagoon	15.14	34.98	0.709168 ± 0.000003	0.00 ± 0.03
C03	North Lagoon	14.50	32.96	0.709182 ± 0.000003	-0.01 ± 0.03
C04	North Lagoon	15.28	34.67	0.709170 ± 0.000003	0.00 ± 0.05
C05	North Lagoon	16.01	34.05	0.709189 ± 0.000003	0.02 ± 0.05
C07	South Lagoon	16.10	56.97	0.709221 ± 0.000004	0.11 ± 0.03
C06	South Lagoon	15.15	63.73	0.709236 ± 0.000003	0.06 ± 0.03
C08	South Lagoon	17.95	93.40	0.709237 ± 0.000003	0.18 ± 0.03
C09	South Lagoon	17.07	65.45	0.709240 ± 0.000003	0.18 ± 0.04
C10	South Lagoon	18.30	84.10	0.709240 ± 0.000003	0.16 ± 0.03
C11	South Lagoon	17.70	85.10	0.709239 ± 0.000003	0.19 ± 0.03
C12	South Lagoon	16.50	94.10	0.709276 ± 0.000005	0.20 ± 0.03
SL9	South Lagoon		113.60	0.709255 ± 0.000003	
SL8	South Lagoon		108.10	0.709249 ± 0.000003	
SL7	South Lagoon		104.65	0.709243 ± 0.000003	
SL6	South Lagoon		89.35	0.709248 ± 0.000003	
SL5C	South Lagoon		82.10	0.709241 ± 0.000003	

SL5B	South Lagoon		81.55	0.709240 ± 0.000003	
SL4B	South Lagoon		83.30	0.709240 ± 0.000003	
SL4A	South Lagoon		85.30	0.709244 ± 0.000003	
SL1B	South Lagoon		82.55	0.709238 ± 0.000003	
SL2	South Lagoon		78.10	0.709241 ± 0.000003	
NL1	North Lagoon		34.44	0.709203 ± 0.000003	
NL2	North Lagoon		19.69	0.709248 ± 0.000003	-0.04 ± 0.03
NL3	North Lagoon		19.50	0.709257 ± 0.000003	
NL4	North Lagoon		20.09	0.709248 ± 0.000003	
NL5	North Lagoon		20.75	0.709248 ± 0.000001	
NL6	North Lagoon		20.82	0.709226 ± 0.000003	
NL7	North Lagoon		23.47	0.709228 ± 0.000003	
NLB1	North Lagoon		27.51	0.709197 ± 0.000003	
NLB3	North Lagoon		28.26	0.709198 ± 0.000003	
NLB4	North Lagoon		29.53	0.709189 ± 0.000003	
NLB5	North Lagoon		32.19	0.709190 ± 0.000003	
NLB6	North Lagoon		34.73	0.709182 ± 0.000003	
NLB11	North Lagoon		34.87	0.709172 ± 0.000003	
NLB15	North Lagoon		35.07	0.709176 ± 0.000003	
Groundwater samples					
JWP2	North Lagoon		1.15	0.709319 ± 0.000003	-0.77 ± 0.03
BWP2	North Lagoon		3.66	0.709281 ± 0.000003	-0.69 ± 0.03
Lower Lakes, river and seawater samples					
C01	Lower Lakes connection	15.17	0.80	0.710880 ± 0.000009	-0.84 ± 0.03
LL1	Lake Albert		1.29	0.710515 ± 0.000003	
LL2	Lake Alexandrina		0.43	0.711006 ± 0.000003	
LL3	Lower Lakes Connection		0.35	0.711134 ± 0.000003	

MR1	Murray River		0.15	0.712124 ± 0.000003	
SL11	Southern Ocean		36.97	0.709172 ± 0.000003	
Fish otoliths samples					
M13-01	Murray Mouth		35.00	0.709224 ± 0.000003	
M13-02	Murray Mouth		35.00	0.709242 ± 0.000003	
M13-14	Murray Mouth		35.00	0.709240 ± 0.000003	
C03-02	North Lagoon		32.96	0.709219 ± 0.000003	-1.76 ± 0.03
C03-04	North Lagoon		32.96	0.709236 ± 0.000003	-1.57 ± 0.03
C03-05	North Lagoon		32.96	0.709229 ± 0.000003	
C04-01	North Lagoon		34.67	0.709249 ± 0.000003	-1.46 ± 0.04
C04-02	North Lagoon		34.67	0.709228 ± 0.000003	
C04-03	North Lagoon		34.67	0.709237 ± 0.000003	
C07-01	South Lagoon		56.97	0.709246 ± 0.000003	
C07-02	South Lagoon		56.97	0.709240 ± 0.000003	-1.73 ± 0.04
C06-02	South Lagoon		63.73	0.709225 ± 0.000003	-1.65 ± 0.02
C06-04	South Lagoon		63.73	0.709251 ± 0.000003	
C08-01	South Lagoon		93.40	0.709252 ± 0.000003	-1.76 ± 0.02
C08-03	South Lagoon		93.40	0.709239 ± 0.000003	
C09-01	South Lagoon		65.45	0.709243 ± 0.000003	-1.76 ± 0.03
C09-02	South Lagoon		65.45	0.709243 ± 0.000003	
C10-01	South Lagoon		84.10	0.709245 ± 0.000003	-1.62 ± 0.03
C10-05	South Lagoon		84.10	0.709246 ± 0.000003	
C11-01	South Lagoon		85.10	0.709238 ± 0.000003	-1.61 ± 0.03
C11-03	South Lagoon		85.10	0.709247 ± 0.000003	
C12-01	South Lagoon		94.10	0.709250 ± 0.000003	-2.00 ± 0.03
C12-02	South Lagoon		94.10	0.709245 ± 0.000003	
C12-03	South Lagoon		94.10	0.709244 ± 0.000003	

Table 2. Table of $^{87}Sr/^{86}Sr$ for micro-drilled otoliths sections, presented as measurements with 2 standard errors. For detailed sampling locations and dates, see Table C1 in Appendix C.

Sample ID	sample weight (mg)	Sr (ng)	$^{87}Sr/^{86}Sr \pm 2se$
C03-03 edge	0.07	70	0.709208 ± 0.000004
C03-03 core	0.065	65	0.709227 ± 0.000004
C10-03 edge	0.022	22	0.709262 ± 0.000004
C10-03 core	0.139	139	0.709242 ± 0.000003

Table 3. Table of $^{87}Sr/^{86}Sr$ for South Australia rainwater samples, presented as measurements with 2 standard errors. For detailed sampling locations and dates, see Table C1 in Appendix C.

Sample ID	$^{87}Sr/^{86}Sr \pm 2se$
Rain-IT (galvanized iron tank)	0.710413 ± 0.000005
Rain-PT (polyethylene tank)	0.710085 ± 0.000056
Rain-A Sr	0.711210 ± 0.000003
Rain-B Sr	0.711537 ± 0.000004

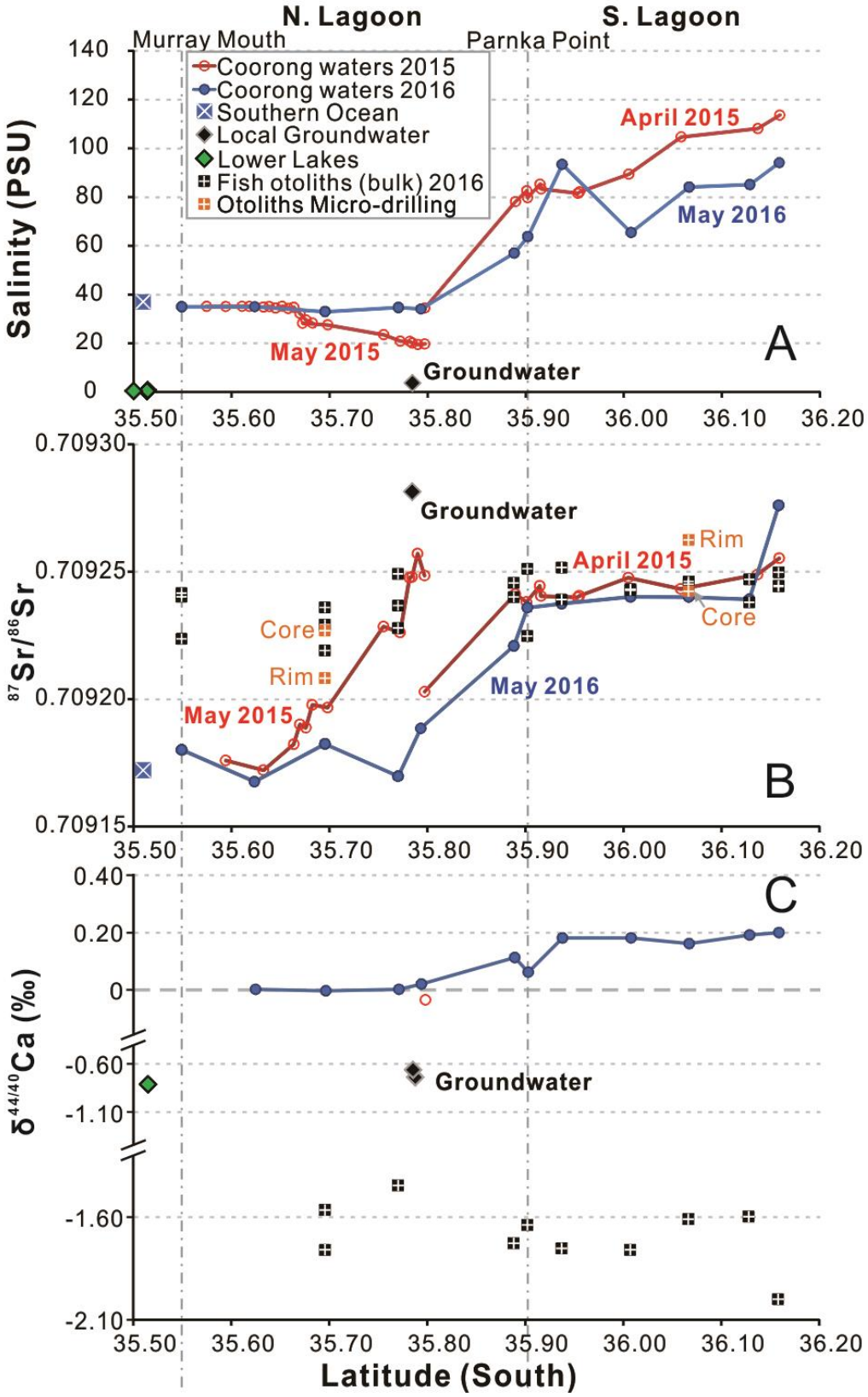

Figure 4: (A) Salinity profile of Coorong Lagoon, from North (left) to South (right), sampled in 2015 and 2016. Solid lines represent trends of water salinity along the lagoon. (B) $^{87}Sr/^{86}Sr$ of water and otolith samples along Coorong Lagoon, fish sampled in 2016 only. Solid lines represent trends of

$^{87}Sr/^{86}Sr$ in water along the lagoon. A black square with white vertical cross represents $^{87}Sr/^{86}Sr$ in a single otolith of one fish; two orange squares with white vertical cross at same latitude represent $^{87}Sr/^{86}Sr$ in core and rim of a single otolith. the Lower Lakes samples are too radiogenic to be plotted on the scale. (C) $\delta^{44}Ca/^{40}Ca$ (i.e. $\delta^{44}Ca$) of waters (circles) and fish otoliths (black squares with white vertical cross) along Coorong Lagoon from brackish/fresh to hypersaline, with rescaled vertical axis.

4.1. The salinity profile through the Coorong lagoons

Generally, the North Lagoon shows similar salinity as Southern Ocean water (~35 PSU), but is followed by a rapid increase in salinity around the narrow connection between North and South Lagoon (i.e. Parnka Point). In contrast, South Lagoon, is a highly restricted part of the Lagoon system, and shows obvious hypersalinity (>70 PSU), with its salinity continuously increasing to the southern end of the lagoon (see Fig. 4A). However, compared with previous studies by Gillanders and Munro (2012) and Webster (2010), the salinity of South Lagoon has become lower over the past decade, decreasing from about 130 PSU in 2003 to less than 100 in 2016, but the salinity of North Lagoon remains relatively constant at around 35 PSU, except for the localised and short-term freshwater input events (Fig. 4A). There are several differences in the salinity profiles between the year 2015 and 2016. Most obviously, the May 2015 data shows an abrupt decrease of salinity from the middle of North Lagoon to Rob's Point (19.69 PSU), where local groundwater was sampled nearby; however, the salinity of water at Rob's Point was near marine salinity (34.45 PSU) in April 2015; (ii) the South Lagoon is about 20 PSU less saline in 2016 than it was in 2015.

4.2. Strontium isotope data ($^{87}Sr/^{86}Sr$)

A total of 72 samples were analysed for Sr isotopes (i.e. $^{87}Sr/^{86}Sr$), including 44 water samples, 28 otoliths or sections of otoliths and 4 rainwater samples (see Fig. 4B).

4.2.1. LAGOON WATERS - STONTIUM ISOTOPE SIGNATURES

The $^{87}Sr/^{86}Sr$ in lagoon waters varied from 0.709168±0.000003 (2 standard errors) in North Lagoon to 0.709276±0.000005 in South Lagoon; the $^{87}Sr/^{86}Sr$ of Southern Ocean water is at the low end, which is 0.709172±0.000003, and the $^{87}Sr/^{86}Sr$ of the groundwater sits above the high end, which is 0.709281±0.000003. The trends of $^{87}Sr/^{86}Sr$ in water along the lagoon show the following features (see also Fig 4B): (i) generally increasing trend to more radiogenic and "non-marine" values from North to South Lagoon, and also (ii) a rapid increase in $^{87}Sr/^{86}Sr$ from the middle of North Lagoon approaching the composition of local groundwaters (sampled at the site). Overall, the $^{87}Sr/^{86}Sr$ signatures of North Lagoon waters are similar to that of typical modern seawater or Southern Ocean waters (0.709172). In contrast $^{87}Sr/^{86}Sr$ in hypersaline South Lagoon waters are much more radiogenic and close to 0.709240.

4.2.2. FISH OTOLITHS - STRONTIUM ISOTOPE SIGNATURES

The $^{87}Sr/^{86}Sr$ of bulk fish otoliths vary from 0.709219±0.000003 in North Lagoon to 0.709252±0.000003 in South Lagoon (see Fig. 4B). There are several interesting patterns in our otolith data: (i) $^{87}Sr/^{86}Sr$ in South Lagoon fish otoliths were very close to the composition of local waters; while (ii) $^{87}Sr/^{86}Sr$ in North Lagoon fish otoliths are systematically more radiogenic than local waters (see Fig 4B), and even comparable to the ratios of South Lagoon fish otoliths.

The $^{87}Sr/^{86}Sr$ of micro-drilled sections of otoliths (see Fig. 5 below) represent average values of different life periods of the fish and therefore $^{87}Sr/^{86}Sr$ history of waters the fish lived in. Generally, the North Lagoon sample (C03-03) was less radiogenic than the South Lagoon sample (C10-10), and there was a larger difference between the $^{87}Sr/^{86}Sr$ of rim samples. However, it is interesting to note that C03-03 has a rim $^{87}Sr/^{86}Sr$ signature that

is closer to the local water, while C10-03 has its core signature closer to the local water and the rim signature more radiogenic. Overall, due to the low mobility of hardyheads and their life span of ca. 1 year, we propose that the bulk otolith $^{87}Sr/^{86}Sr$ data represent a good approximation of the long-term (i.e., 1 year) average Sr isotope composition of the nearby lagoon waters (i.e., in the vicinity of the specific sites where the fish samples were collected).

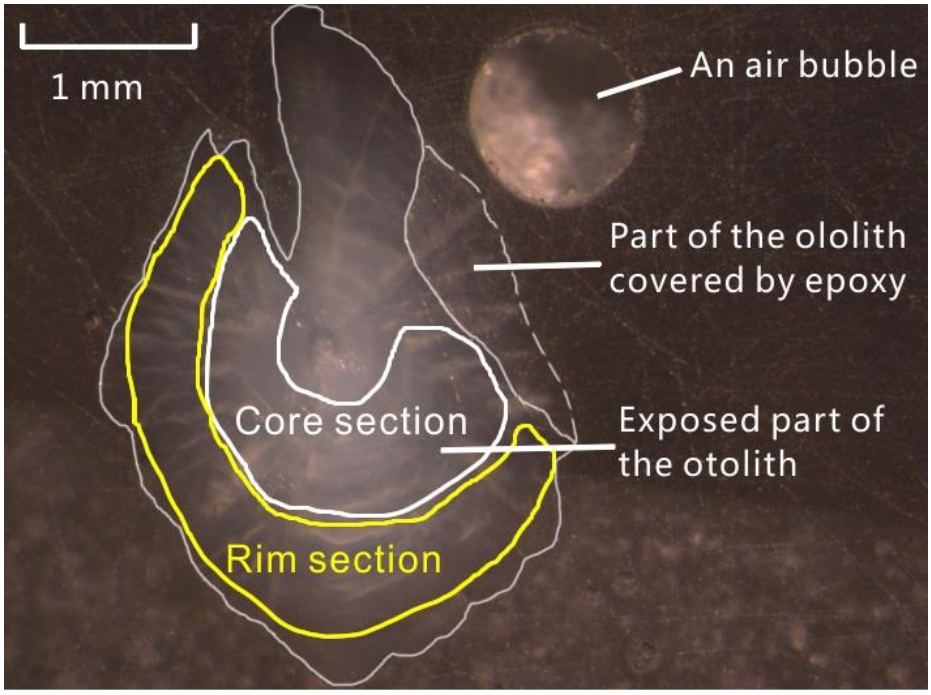

Figure 5: Photo of otolith sample C03-03 embedded in epoxy and polished, with micro-drilling section patterns on the exposed part of the otolith indicated.

4.2.3. LOCAL RAINWATER - STRONTIUM ISOTOPE SIGNATURES

Our samples of local South Australian atmospheric deposition (i.e., rainwater) show rather radiogenic $^{87}Sr/^{86}Sr$ signatures (see data in Table 3), and unlike any Coorong Lagoon samples, they are closer to the composition of Lower Lakes and Murray River signatures. In additoin, rainwaters accumulated over several years, Rain-IT and Rain-PT, show less radiogenic signatures than the 29th-30th August 2016 rainwaters (i.e. Rain-A

and Rain-B). Overall, the rainwaters yielded $^{87}Sr/^{86}Sr$ signatures that range from 0.710413 up to 0.711537 (cf., Table 3).

4.3. Calcium isotope data ($\delta^{44/40}Ca$)

A total of 25 samples were analysed for Ca isotopes (i.e. $\delta^{44/40}Ca$), including 15 water samples and 10 bulk otoliths (see Fig. 4C).

4.3.1. LAGOON WATERS - CALCIUM ISOTOPE SIGNATURES

The $\delta^{44/40}Ca$ of the lagoon waters generally increased with the increasing salinity (see Fig. 4C), with the exception of a site near where local groundwater input was detected and salinity was lower (i.e., near the site of Noonameena where local groundwaters were collected). The normal marine samples with salinities close to 35 PSU, collected within North Lagoon, have $\delta^{44/40}Ca$ values close to 0‰ (i.e., identical with modern seawater), while brackish/fresh water samples have values as negative as -0.85‰ (including the groundwater samples and the Lower Lake sample). As mentioned, the exception is the North Lagoon brackish sample (with salinity of 20 PSU), which has a $\delta^{44/40}Ca$ value just below 0‰; and also the hypersaline samples in South Lagoon that show $\delta^{44/40}Ca$ values systematically above 0‰, where the signatures increase with salinity up to $\delta^{44/40}Ca$ about 0.20‰ (see Fig. 4C).

4.3.2. FISH OTOLITHS - CALCIUM ISOTOPE SIGNATURES

Overall, the fish otolith samples yielded very negative $\delta^{44/40}Ca$ values (relative to seawater and/or local lagoon waters) with an average of about -1.60‰, ranging from -2.00 to -1.46‰. There is also no systematic correlation between the $\delta^{44/40}Ca$ signatures of otoliths and local lagoon waters (see Fig. C2 in Appendix C), indicating that

biomineralisation processes rather than *water mixing* are primarily responsible for the observed variability in the Ca isotope composition of the otoliths.

5. DISCUSSION

5.1. The salinity profile in the Coorong lagoon system

Given that the lagoon water exchanges with the Southern Ocean through the Murray Mouth, and its exchange with the Lower Lakes is limited by artificial barrages, and the restricted condition of the South Lagoon, the highly notable difference in salinity between North and South Lagoon could be the result of: (i) high evaporation rate in South Lagoon due to its isolation from other water bodies, and/or (ii) restricted input of ocean water into South Lagoon through Parnka Point. The effect of water leakage through the artificial barrages seems limited, since there was no obvious decrease or oscillations in salinity near the Murray Mouth.

As to annual variability, there are several possible causes for the observed difference of ca. 20 PSU in salinity of South Lagoon waters as measured during 2015 and 2016 (see Fig. 4A). These include: (i) increased local precipitation and input of fresh rainwater or groundwater into South Lagoon in 2016; (ii) decreased water evaporation in South Lagoon; and/or (iii) continuous limitation of ocean water input into South Lagoon through Parnka Point. Based on the salinity profiles and the fact that North Lagoon has more active interaction with Southern Ocean, it seems more plausible that the observed drop in salinity in South Lagoon during 2016 is likely due to decrease in water evaopration, combined with increased inputs of rainwater and/or groundwater, which can be tested through $^{87}Sr/^{86}Sr$ proxy.

There are also other possible freshwater inputs to the lagoon that can be considered such as Lower Lakes water leakage through the barrages, but based on the location of this abrupt salinity decrease, the effect of water leakage through the barrages should be relatively minimal, since no obvious decrease in salinity around the northern end of the lagoon was observed. Also, if local precipitation and rainwater inputs have a significant impact, rather than local groundwater inputs, then the decrease in salinity should be more homogeneous along the North Lagoon than it actually is, and such a steep decline in salinity from latitudes 35.66 to 35.69 degrees should not be seen.

5.2. The Sr isotope systematics in the Coorong lagoons and Murray Mouth

5.2.1. THE STRONTIUM ISOTOPE PROFILE AND WATER MIXING

5.2.1.1. The Sr isotope profile across the Coorong lagoons

The $^{87}Sr/^{86}Sr$ ratio, as a powerful indicator of distinct water sources, is used here to indicate the most significant water inputs into the lagoons. The possible sources of water inputs are: (i) Southern Ocean water; (ii) local groundwater; (iii) Murray River water; and (iv) rainwater. Based on the generated $^{87}Sr/^{86}Sr$ profile across the lagoons (Fig. 4B), the most obvious feature is the distinctive and systematic difference in $^{87}Sr/^{86}Sr$ between North and South Lagoon, which indicates different dominant water sources for these two parts of the Coorong Lagoon system. Specifically, based on $^{87}Sr/^{86}Sr$ data, the North Lagoon waters are largely sourced from Southern Ocean, whereas the South Lagoon waters also originated from the continental and more radiogenic Sr sources, such as local groundwater, river waters and/or rainwaters. Moreover, the similar radiogenic $^{87}Sr/^{86}Sr$ values in South Lagoon observed for 2015 and 2016 confirmed that the source of water is likely the same continental input mixing with ocean water; and the salinity decline in

2016 is likely a result of the decline in evaporation rate during 2016. The groundwater input in North Lagoon discovered in May 2015 is considered a short-lived event, when more radiogenic $^{87}Sr/^{86}Sr$ derived from local groundwater sources (close to 0.70928) shifted temporarily the $^{87}Sr/^{86}Sr$ of North Lagoon waters to more radiogenic values, as observed in 2015 (see Fig. 4B).

5.2.1.2. Quantification of Sr inputs in lagoon waters and otoliths

By applying the isotopic mass balance equation for Sr, using $^{87}Sr/^{86}Sr$ signatures of water and otolith samples, the relative contribution of different water sources can be calculated (cf., Kell-Duivestein (2015),. Here, seawater and ground water sources are considered as the two major sources of Sr into the lagoon system, in other words, the lagoon samples are considered as mixtures of these two, and the otolith signatures are considered as bulk estimates or long-term averaged values for water signatures throughout several months up to a year (i.e., the life span of hardyhead fish species).
The isotopic mass balance equation of Sr is expressed below:

$$^{87}Sr/^{86}Sr_{\,sample} = {}^{87}Sr/^{86}Sr_{\,SW} \cdot F_{SW} + {}^{87}Sr/^{86}Sr_{\,GW} \cdot (1 - F_{SW}) \qquad \text{(Eq. 2)}$$

Where $^{87}Sr/^{86}Sr_{\,sample}$ is the $^{87}Sr/^{86}Sr$ signature of the water or otolith sample; $^{87}Sr/^{86}Sr_{\,SW}$ is the $^{87}Sr/^{86}Sr$ signature of the South Ocean water, which is 0.70917; $^{87}Sr/^{86}Sr_{\,GW}$ is the $^{87}Sr/^{86}Sr$ signature of the local groundwater (sampled in 2015) which is 0.70930 (Kell-Duivestein, 2015). Finally, F_{SW} is the fraction of seawater-derived Sr into the lagoon.

Based on Eq. 2, the relationship between $^{87}Sr/^{86}Sr_{\,sample}$ and F_{SW} can be plotted as an inverse linear relationship (see Fig. 6).

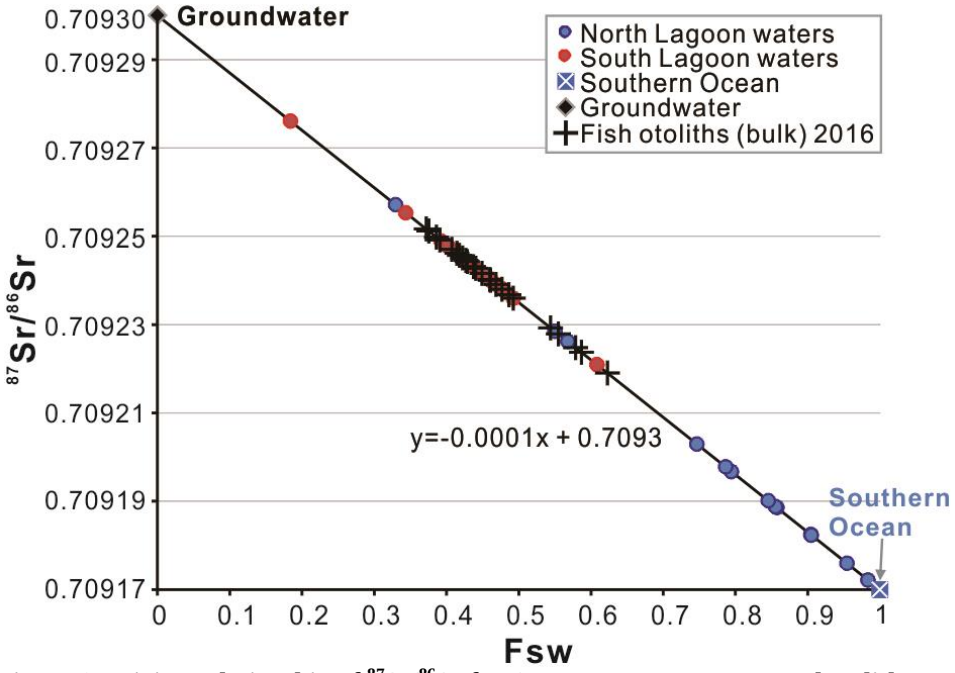

Figure 6: Mixing relationship of $^{87}Sr/^{86}Sr$ for Coorong Lagoon water and otoliths samples as a result of interaction between groundwater and seawater endmembers, plotted as $^{87}Sr/^{86}Sr$ vs. the fraction of seawater input F_{SW}.

The fractions of seawater-derived Sr for each sample of lagoon water and/or otolith can be calculated using the Eq. 2, and the mixing trend is plotted in Fig. 6. Note that the fraction of the groundwater-derived Sr input (F_{GW}) can be calculated by $F_{GW} = 1 - F_{SW}$. The calculated fractions of F_{SW} and F_{GW} for our samples are shown below in Table 4.

Table 4. Calculated fractions of Sr input from groundwater and seawater to account for $^{87}Sr/^{86}Sr$ of the 2016 samples using mass balance equation of Sr.

Sample ID	Area	$^{87}Sr/^{86}Sr$	2sem	F_{SW}	F_{GW}
Lagoon water samples					
C02	North Lagoon	0.709168	0.000003	1.00	0.00
C03	North Lagoon	0.709182	0.000003	0.90	0.10
C04	North Lagoon	0.709170	0.000003	1.00	0.00
C05	North Lagoon	0.709189	0.000003	0.86	0.14
NL1	North Lagoon	0.709203	0.000003	0.75	0.25
NL2	North Lagoon	0.709248	0.000003	0.40	0.60
NL3	North Lagoon	0.709257	0.000003	0.33	0.67
NL4	North Lagoon	0.709248	0.000003	0.40	0.60
NL5	North Lagoon	0.709248	0.000001	0.40	0.60
NL6	North Lagoon	0.709226	0.000003	0.57	0.43
NL7	North Lagoon	0.709228	0.000003	0.55	0.45
NLB1	North Lagoon	0.709197	0.000003	0.79	0.21
NLB3	North Lagoon	0.709198	0.000003	0.79	0.21

NLB4	North Lagoon	0.709189	0.000003	0.86	0.14
NLB5	North Lagoon	0.709190	0.000003	0.85	0.15
NLB6	North Lagoon	0.709182	0.000003	0.91	0.09
NLB11	North Lagoon	0.709172	0.000003	0.98	0.02
NLB15	North Lagoon	0.709176	0.000003	0.95	0.05
C07	South Lagoon	0.709221	0.000004	0.61	0.39
C06	South Lagoon	0.709236	0.000003	0.49	0.51
C08	South Lagoon	0.709237	0.000003	0.48	0.52
C09	South Lagoon	0.709240	0.000003	0.46	0.54
C10	South Lagoon	0.709240	0.000003	0.46	0.54
C11	South Lagoon	0.709239	0.000003	0.47	0.53
C12	South Lagoon	0.709276	0.000005	0.18	0.82
SL9	South Lagoon	0.709255	0.000003	0.34	0.66
SL8	South Lagoon	0.709249	0.000003	0.39	0.61
SL7	South Lagoon	0.709243	0.000003	0.44	0.56
SL6	South Lagoon	0.709248	0.000003	0.40	0.60
SL5C	South Lagoon	0.709241	0.000003	0.46	0.54
SL5B	South Lagoon	0.709240	0.000003	0.46	0.54
SL4B	South Lagoon	0.709240	0.000003	0.46	0.54
SL4A	South Lagoon	0.709244	0.000003	0.43	0.57
SL1B	South Lagoon	0.709238	0.000003	0.48	0.52
SL2	South Lagoon	0.709241	0.000003	0.45	0.55
Fish otoliths					
M-01	Murray Mouth	0.709224	0.000003	0.59	0.41
M-02	Murray Mouth	0.709242	0.000003	0.45	0.55
M-14	Murray Mouth	0.709240	0.000003	0.46	0.54
C03	North Lagoon	0.709219	0.000003	0.62	0.38
C03	North Lagoon	0.709236	0.000003	0.49	0.51
C03	North Lagoon	0.709229	0.000003	0.54	0.46
C04	North Lagoon	0.709228	0.000003	0.55	0.45
C04	North Lagoon	0.709237	0.000003	0.49	0.51
C04	North Lagoon	0.709249	0.000003	0.39	0.61
C07	South Lagoon	0.709240	0.000003	0.46	0.54
C07	South Lagoon	0.709246	0.000003	0.42	0.58
C06	South Lagoon	0.709225	0.000003	0.58	0.42
C06	South Lagoon	0.709251	0.000003	0.38	0.62
C08	South Lagoon	0.709252	0.000003	0.37	0.63
C08	South Lagoon	0.709239	0.000003	0.47	0.53
C09	South Lagoon	0.709243	0.000003	0.44	0.56
C09	South Lagoon	0.709243	0.000003	0.44	0.56
C10	South Lagoon	0.709245	0.000003	0.42	0.58
C10	South Lagoon	0.709246	0.000003	0.41	0.59
C11	South Lagoon	0.709247	0.000003	0.41	0.59

C11	South Lagoon	0.709238	0.000003	0.48	0.52
C12	South Lagoon	0.709250	0.000003	0.39	0.61
C12	South Lagoon	0.709245	0.000003	0.43	0.57
C12	South Lagoon	0.709244	0.000003	0.43	0.57

Based on our simple mass-balance calculations, the proportion of groundwater input in South Lagoon is generally increasing from north to south, with the highest $^{87}Sr/^{86}Sr$ value of about 0.709276 measured in 2016 in a water sample from the most southern tip of the lagoon. The latter might indicate that most of the groundwater entered the lagoon from aquifers south to the lagoon, but the reason for this very radiogenic signature south to Salt Creek could be also due to an additional input of radiogenic Sr from local atmospheric deposition that has quite radiogenic $^{87}Sr/^{86}Sr$ ranging from 0.710413 up to 0.711537 (see data in Table 3).

5.2.2. THE STRONTIUM ISOTOPE SIGNATURES OF OTOLITHS

As hardyheads (*A. microstoma*) have a low mobility and lifespan of about 1 year (Gillanders & Munro, 2012; Wedderburn et al., 2014), the observed and systematically more radiogenic $^{87}Sr/^{86}Sr$ signatures of the otoliths (relative to local lagoon waters, Fig 4B) might be interpreted as a reflection of an integrated long-term signal of local lagoon waters. Accordingly, the otolith data would indicate that there is an overall higher inputs of groundwater Sr sources into the lagoon (over the one-year period) near the sampling sites (as can be seen in Fig. 6), compared to estimates that are based on "snap-shot" sampling of lagoon waters performed in 2015 and 2016. Also, the otoliths $^{87}Sr/^{86}Sr$ signatures are generally closer to water signatures collected in 2015, or plot between 2015 and 2016 water data (Fig. 4B), which is consistent with the proposed concept of ca. 1-year integration of water signatures being reflected in otoliths.

It is notable that otolith $^{87}Sr/^{86}Sr$ signatures at the Murray Mouth do not match with the local water signature (Fig. 4B), which is surprising given that the Murray Mouth is where ocean water enters the lagoon. Therefore, local water and otolith signatures were both expected to be very close to seawater or Southern Ocean $^{87}Sr/^{86}Sr$ signature, and stay relatively stable over time, assuming that hardyheads indeed do not migrate significantly. A possible reason for the observed difference between $^{87}Sr/^{86}Sr$ of waters and otoliths at the Murray Mouth could be a water leakage from the Lower Lakes through the barrages, which brought radiogenic signals to the fish in the vicinity.

As to the rest of the Coorong lagoon system, compared with North Lagoon where the hydrodynamics is more complicated, the South Lagoon water $^{87}Sr/^{86}Sr$ signatures are relatively well reflected by the otoliths, and hence the otolith Sr isotope signatures can be considered as an intergrated average values of local water over the fish's lifetime (i.e., about 1 year).

Finally, the micro-drilled sections of the otoliths can be considered as averages of early and recent stages $^{87}Sr/^{86}Sr$ incorporated by the fish. Sample C03-03 shows the recent $^{87}Sr/^{86}Sr$ signature was less radiogenic than its early life, which matches the decline in water $^{87}Sr/^{86}Sr$ signature over one year. Sample C10-03, on the other hand, shows that the recent $^{87}Sr/^{86}Sr$ signature has combined some radiogenic water, likely carried from the southern end of the lagoon, and the early $^{87}Sr/^{86}Sr$ signature was similar to the water signature in 2015.

5.2.3. LOCAL RAINWATER STRONTIUM ISOTOPE SIGNATURES

Our rainwater samples, collected in Adelaide area, have to be considered as approximate estimates of South Australia local precipitation, as they were collected more than 100 km away from the Coorong lagoon. Thus, their $^{87}Sr/^{86}Sr$ signatures may not be

fully representative of a local precipitation at the Coorong. Nevertheless, they serve as a good proxy for local atmospheric deposition and its Sr isotope signature. Considering the high rainfall and precipitation in 2016, the calculated fractions of groundwater inputs into the lagoon (see Table 3) are likely slightly overestimated, because the rainwater $^{87}Sr/^{86}Sr$ signatures are also radiogenic, although the Sr concentration in rainwater is very low. Additionally, the radiogenic $^{87}Sr/^{86}Sr$ of local rainwater might explain the exceptionally radiogenic $^{87}Sr/^{86}Sr$ signature south to Salt Creek, as more rainwater can be drained into the lagoon through Upper Southeast Drainage area (USED) at the southern end of the lagoon. Overall, the impact from rainwater is difficult to quantify with our data, but due to the similarity of lagoon water $^{87}Sr/^{86}Sr$ signatures between year 2015 and 2016, it is expected that annual changes in rainfall are unlikely to significantly affect the Sr isotope budget of the lagoon waters, but the effect of rainfall on $^{87}Sr/^{86}Sr$ signatures of lagoon water can be cumulative over the longer periods, shifting them gradually to more radiogenic values.

5.3. The Ca isotope systematics in the Coorong lagoons and Murray Mouth

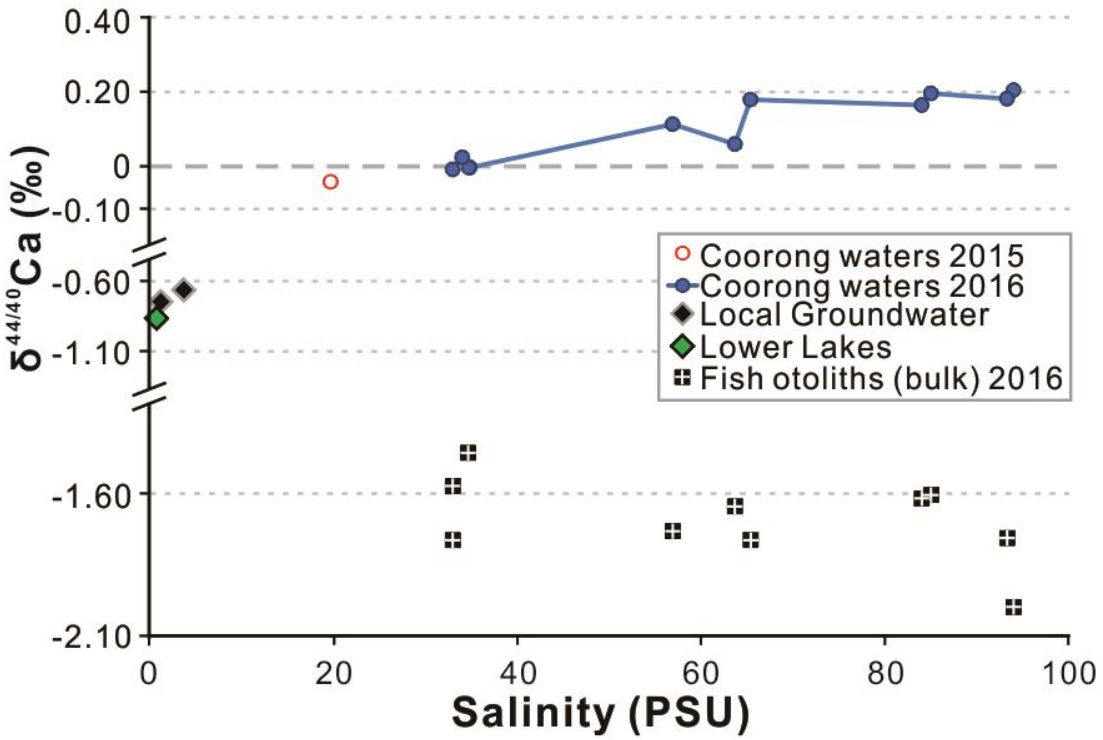

Figure 7: $\delta^{44}Ca/^{40}Ca$ (i.e. $\delta^{44}Ca$) of waters (circles) and fish otoliths (black squares with white vertical cross) vs. salinity (PSU) along Coorong Lagoon from brackish/fresh to hypersaline. The $\delta^{44/40}Ca$ values were normalised to standard seawater.

5.3.1. LAGOON WATERS - CALCIUM ISOTOPE SIGNATURES

5.3.1.1. North Lagoon $\delta^{44/40}Ca$ profile

After plotting $\delta^{44/40}Ca$ against salinity (PSU), we can see a general increasing trend of $\delta^{44/40}Ca$ with salinity (Fig 7). Based on Fig. 2, from Fantle and Tipper (2014), the rivers and rainwaters, which are brackish/fresh, have lower $\delta^{44/40}Ca$ values than seawater, this matches with $\delta^{44/40}Ca$ values of groundwater and Lower Lakes samples analysed here. Accordingly, the brackish sample in North Lagoon can be considered as a mixing product of the seawater end member and the groundwater member. The mixing follows the rule of chemical compositions of two-component mixtures, described by Faure (1977); in this case it is expressed as:

$$\delta^{44/40}Ca_{sample} = \delta^{44/40}Ca_{SW} \cdot F_{SW} + \delta^{44/40}Ca_{GW} \cdot (1 - F_{SW}) \quad \text{(Eq. 3.1)}$$

where F_{SW} is the seawater-derived fraction of Ca input into the lagoon waters.

To quantify this Ca input, the formula can be transformed into:

$$F_{SW} = \frac{\delta^{44/40}Ca_{sample} - \delta^{44/40}Ca_{GW}}{\delta^{44}/40Ca_{SW} - \delta^{44/40}Ca_{GW}} \quad \text{(Eq. 3.2)}$$

Based on this equation, the seawater-derived fraction of Ca (F_{SW}) in the sample NL2 (i.e., the brackish North Lagoon sample) is calculated to be close to 0.95 (95%), with the remaining 5% of Ca originating from groundwater sources. This calculated partitioning between seawater and groundwater Ca sources for the sample NL2 is different from the estimates based on Sr isotope mass balance (data in Kell-Duivestein (2015) which suggest that about 60% of Sr in NL2 was derived from local groundwater. This discrepancy between Sr and Ca isotope mass balance approaches could be explained by the fact that unlike radiogenic Sr isotopes, the stable Ca isotopes in waters are also impacted by the precipitation of carbonates in the lagoon system (see below). Alternatively, if one assumes that NL2 is the product of mixing between groundwater and the South Lagoon waters with Sr and Ca isotope signatures of 0.709248 ± 0.000003 and +0.20 ± 0.03‰, then the calculated groundwater fractions are closer: i.e. 15% for Sr and 25% for Ca mass balance.

5.3.1.2. South Lagoon δ44/40Ca profile

Modern seawater has the heaviest $\delta^{44/40}$Ca signature from major near-surface Ca reservoirs (see Fig. 2). However, the hypersaline South Lagoon waters have $\delta^{44/40}$Ca signatures that are even heavier than typical seawater by up to ~0.2‰ (Fig 4C). Thus, these anomalously heavy $\delta^{44/40}$Ca values cannot be explained by a simple mixing of the two end members: i.e. seawater and groundwater with $\delta^{44/40}$Ca signatures of 0 and -0.77‰ (see Table 1), respectively. The heavy $\delta^{44/40}$Ca values of South Lagoon waters can,

however, be explained by the ongoing precipitation of $CaCO_3$ mineral phases in the lagoon, as the formation of calcite and aragonite preferentially removes light ^{40}Ca isotopes from the solution (Gussone et al., 2005), leaving the remaining fluid (i.e., lagoon water) enriched in heavy Ca isotopes, thus with heavy $\delta^{44/40}Ca$ values. According to von der Borch et al. (1975), carbonates precipitated from the Coorong lagoon are mainly aragonite (90-95%) and calcite (5-10%), and thus to interpret our heavy $\delta^{44/40}Ca$ water data from South Lagoon we need to consider the precipitation of these two $CaCO_3$ polymorphs. Gillanders and Munro (2012) also pointed out that precipitation of carbonates (especially aragonite) possibly starts when the brine reaches twice the concentration of seawater (40-60 PSU salinity), based on their progressively more scattered Ca and Sr concentration data of Coorong Lagoon waters at higher salinities.

5.3.1.2.1. Quantifying Ca removal and carbonate ($CaCO_3$) output in South Coorong Lagoon

However, in our calculations of possible carbonate ($CaCO_3$) output flux in South Lagoon, based on Ca isotope data, we need to also consider the fact that South Lagoon receives a certain amount of seawater and groundwater-derived Ca supply through North Lagoon and groundwater discharge. Thus, two models are used here (open vs. closed system) as plausible end member scenarios to explain the positive $\delta^{44/40}Ca$ values of South Lagoon waters, and to quantify the relative precipitation and output flux of carbonates in the lagoon:

1) The closed system Rayleigh fractionation model

Assuming no extra water supply to South Lagoon, in another words, a closed system, the Rayleigh fractionation model can be used to describe the partitioning of Ca isotopes

between two reservoirs (i.e. lagoon water and carbonate) while the lighter ^{40}Ca is continuously removed from the lagoon waters to form carbonates, and the Ca isotopic composition in the residuals (i.e. lagoon waters) can be calculated based on:

$$\delta^{44/40}Ca = \left[\left(\delta^{44/40}Ca_{ini} + 10^3\right)(1-f)^{(\alpha-1)}\right] - 10^3 \quad \text{(Eq. 4.1)}$$

where $\delta^{44/40}Ca$ is the signature of the residual lagoon water;

$\delta^{44/40}Ca_{ini}$ is the signature of lagoon water at the time of zero carbonate precipitation;

f is the fraction of Ca in removed as carbonates; and α is the fractionation factor (i.e., the difference between $\delta^{44/40}Ca$ of mineral = $CaCO_3$ and fluid = lagoon water), which stays constant during the entire process.

For calculating $\delta^{44/40}Ca_{ini,}$ based on $^{87}Sr/^{86}Sr$ mixing model, the ratio of groundwater input to South Lagoon has been quantified as 60-65% if there was no carbonate precipitation, and by applying these constraints and mass balance mixing on $\delta^{44/40}Ca$, the estimated $\delta^{44/40}Ca_{ini}$ was calculated to be ~-0.45‰, due to the contribution of isotopically light Ca from the groundwater sources (see also Eq. 3.1)

The α can be calculated by $\alpha = R_{prod}/R_{react}$, where R_{prod} and R_{react} are the $^{44}Ca/^{40}Car$ ratios of the carbonate precipitated and the lagoon water, respectively. Alternatively, the parameter α can be also expressed as: $\alpha = \frac{1+\frac{\delta^{44/40}Ca_{prod}}{1000}}{1+\frac{\delta^{44/40}Ca_{react}}{1000}} = \frac{1000+\delta^{44/40}Ca_{prod}}{1000+\delta^{44/40}Ca_{react}}$, where $\delta^{44/40}Ca_{prod}$ refers to $\delta^{44/40}Ca$ of the carbonate precipitated, which are -1.5‰ and -0.9‰ for aragonite and calcite respectively (Gussone et al. (2005); and $\delta^{44/40}Ca_{react}$ refers to $\delta^{44/40}Ca$ of seawater, which is 0‰.

To calculate f (i.e., the fraction of Ca removed from the lagoon system as carbonate), we can rewrite Eq. 4.1 as:

$$f = 1 - \sqrt[\alpha-1]{\frac{\delta^{44}Ca+10^3}{\delta^{44}Ca_{ini}+10^3}} \quad \text{(Eq. 4.2)}$$

As a result, the relative quantification of carbonate precipitation in the South Coorong lagoon, for a closed system scenario, is modeled below (see Fig. 8).

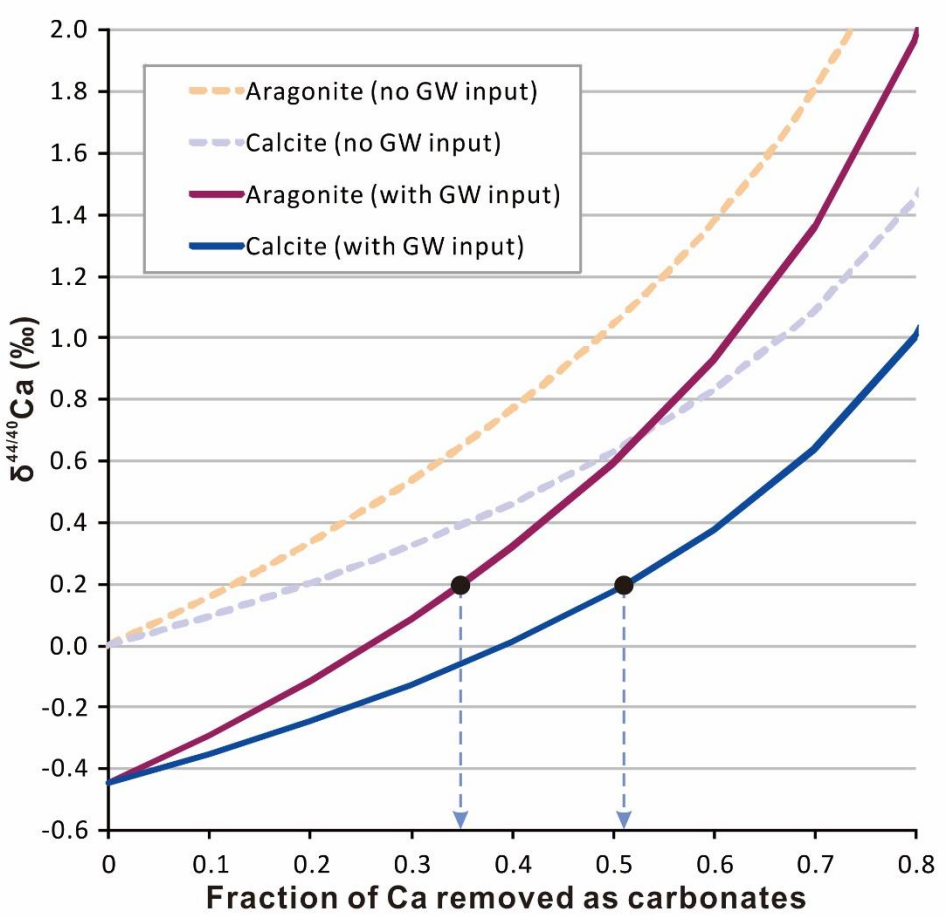

Figure 8: The closed system/Rayleigh fractionation model of water mixing and carbonate precipitation in South Lagoon, assuming no external water supply, and precipitates are mainly aragonite and calcite. The groundwater input was estimated as 60-65% based on $^{87}Sr/^{86}Sr$ mixing constraints.

Based on modeling presented in Fig. 8 (i.e., solid lines scenarios), and heavy $\delta^{44/40}Ca$ signatures of South lagoon waters (up to +0.2 ‰), we estimated that approximately 35 to 50% of Ca in South Lagoon was removed as $CaCO_3$, depending on the mineralogy, and because most of these precipitates are aragonite (von der Borch et al., 1975), this value would be closer to 35%.

2) The open system or steady-state fractionation model

In this model, we assume the rate of external Ca input to South Lagoon (i.e., from North Lagoon) to be the same as the rate of Ca output (i.e. precipitating as carbonates) such that

the Ca concentration of the reactant (i.e. lagoon water) keeps constant, as a consequence, the rate of Ca isotope fractionation stays constant.

Modified from Frings et al. (2016), the Ca isotopic composition in the residual reservoir (i.e. lagoon waters) can be expressed as:

$$\delta^{44/40}Ca = \varepsilon \cdot f + \delta^{44/40}Ca_{ini} \quad \text{(Eq. 5.1)}$$

where $\delta^{44/40}Ca$ is the signature of the residual lagoon water;

ε is the fractionation factor between seawater and carbonate mineral presented in ‰, can be calculated from the equation $\varepsilon = 10^3(\alpha - 1)$, the values for aragonite and calcite are 1.5‰ and 0.9‰ respectively.

f is the fraction of Ca in removed as carbonates;

$\delta^{44/40}Ca_{ini}$ is the signature of lagoon water at the time of zero carbonate precipitation, which is calculated to be the same as for the closed system model (i.e. -0.45‰).

To calculate f (i.e., the fraction of Ca in removed from the system as carbonate), we rewrite Eq. 5.1 as:

$$f = \frac{\delta^{44/40}Ca - \delta^{44/40}Ca_{ini}}{\varepsilon} \quad \text{(Eq. 5.2)}$$

In a similar way, the relative quantification of carbonate precipitation for an open system scenario (i.e., the South Lagoon communicated with North Lagoon) is modeled below (Fig. 9).

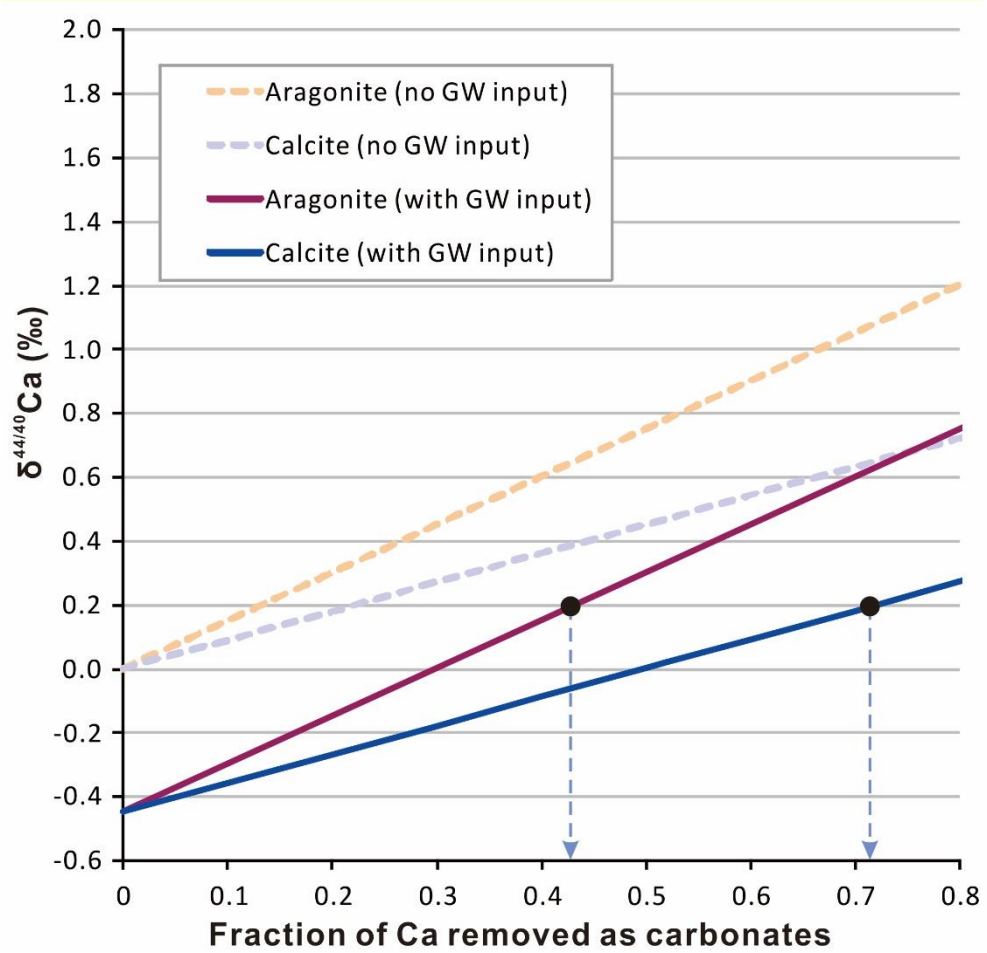

Figure 9: The open system/steady-state model of water mixing and carbonate precipitation in South Lagoon, assuming constant Ca concentration in lagoon water, and precipitates are mainly aragonite and calcite. The groundwater input was estimated as 60-65% based on $^{87}Sr/^{86}Sr$ mixing.

Based on Fig. 9 (i.e., solid lines), we estimate that about 40 to 70% Ca had to be removed as $CaCO_3$ in South Lagoon, to explain the heavy $\delta^{44/40}Ca$ signatures of local lagoon waters (+0.2 ‰), and because most of the carbonate precipitates in the Coorong lagoons are aragonites (von der Borch et al., 1975), this value would be closer to 40%.

In conclusion, based on these two models, the range of fraction of Ca removed as carbonates (mostly aragonite) in South Coorong lagoon is estimated to be from 35 to 40% (i.e., closed vs. open system scenarios, respectively).

5.3.2. OTOLITHS CALCIUM ISOTOPE SIGNATURES

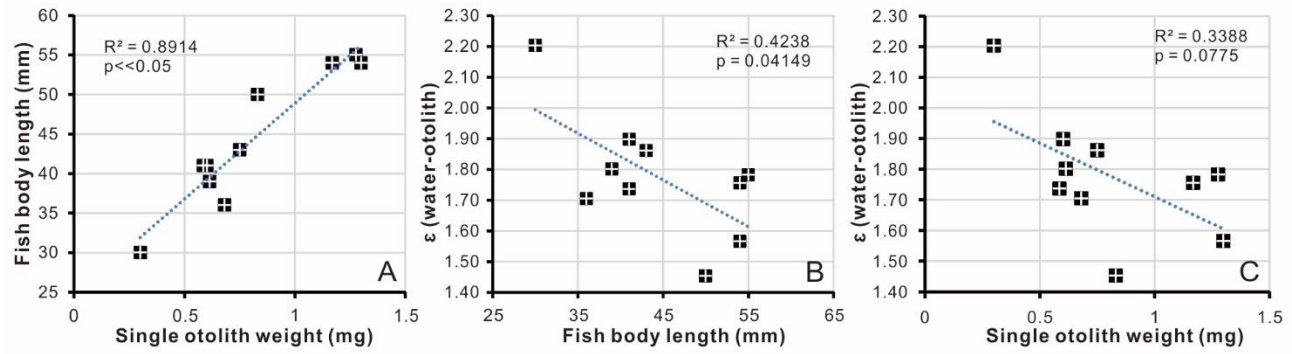

Figure 10: Correlations of fish size parameters (i.e. Fish body length and single otoliths weight) with otoliths $\delta^{44/40}$Ca values: (A) Fish body length vs. single otoliths weight; (B) Fractionation factor ε of $\delta^{44/40}$Ca between lagoon water and otoliths of the same sampling site vs. fish body lengths; (C) Fractionation factor ε vs. single otoliths weight. In chart (B) and (C), $\delta^{44/40}$Ca for sites C07, C08 and C09 in South Lagoon were estimated by linear interpolation of $\delta^{44/40}$Ca between the most proximal sites, and ε values were then calculated.

The $\delta^{44/40}$Ca values of fish otoliths do not directly reflect water sources but rather may reflect biologically controlled fractionation processes (see Figs. 4C and 7). Overall, otolith $\delta^{44/40}$Ca data are systematically lighter than those in local waters, confirming that during the otoliths formation the light Ca isotopes are preferentially incorporated during the growth (i.e., the formation of aragonite from core to rim of otoliths). Although not related to water signatures, $\delta^{44/40}$Ca of otoliths differentiated among fish of different sizes as a result of Ca isotope fractionation during growth of the otoliths. To better visualise the fractionation of Ca isotope from ambient water, the fractionation factor ε, which is the difference in $\delta^{44/40}$Ca signatures between water and otolith samples, is plotted against the fish size parameters (Fig. 10). Specifically, it is obvious that the size of otoliths is proportional to the fish body length according to high R^2 (0.8914) and low p (<<0.05) values; but also in general, the large (more mature) fish yield smaller fractionations in otoliths, while small (juvenile) fish yielded larger fractionations, although the R^2 and p values are both marginally significant. This overall trends and coupling between Ca isotope fractionations in otoliths and fish ontogeny (i.e., juvenile vs. mature) can be

explained by kinetic isotope fractionation effects, where juvenile fish otoliths might grow at faster rates during early life stages, thus preferentially incorporating lighter Ca isotopes (cf., Fantle and Tipper, 2014), therefore producing larger isotope fractionations. It is also obvious that more mature and larger fish show greater variation in isotope fractionation in otolith; this is possibly because those otoliths recorded a longer history of the fish movement within the lagoon and/or fish growth slows as they age, which caused higher variations in their $\delta^{44/40}$Ca signals, but our preliminary data from fish otoliths are very limited and thus any conclusions presented here must be validated by future and more detail studies. Nevertheless, the available $\delta^{44/40}$Ca data from otoliths suggest an overall strong biological control on otoliths Ca isotope systematics, likely controlled by "kinetic" processes related to changes in fish growth rates. As elemental/Ca concentration patterns in fish otoliths are also sensitive to biological processes (Gillanders & Munro, 2012), future Ca isotopes studies coupled with elemental proxies might help to differentiate signals originating from (i) biological processes (i.e., changes in growth or precipitation rates of otoliths), and those imparted by (ii) distinct water masses with unique elemental and isotope signatures (i.e., fish migration signal).

6. CONCLUSIONS

- The water chemistry of Coorong Lagoon can be considered as mixing of three major components (i.e. the groundwater, seawater/normal marine water and hypersaline water) as shown in Fig. 11A and 11B below, indicated by both $^{87}Sr/^{86}Sr$ and $\delta^{44/40}$Ca signatures.

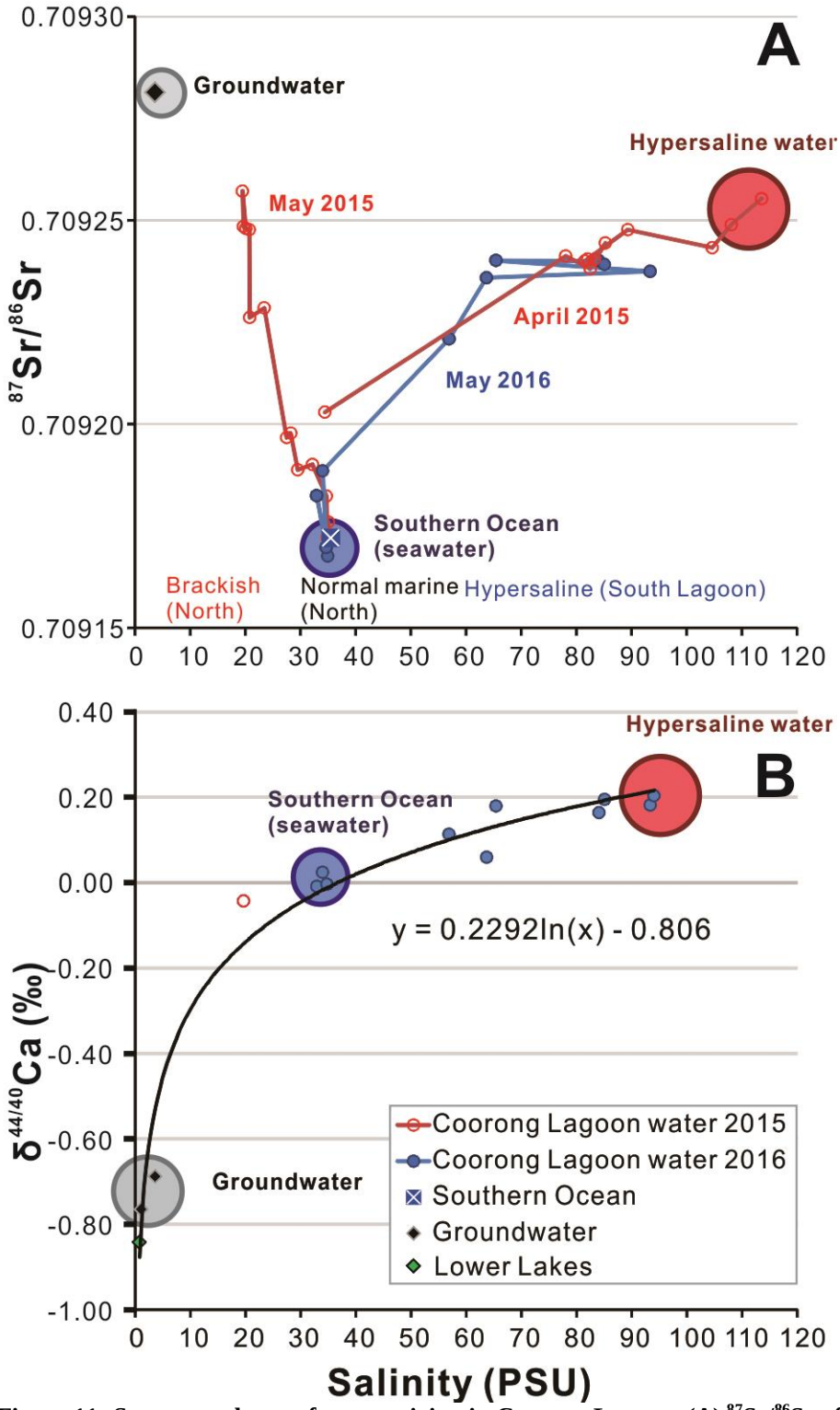

Figure 11: Summary charts of water mixing in Coorong Lagoon: (A) $^{87}Sr/^{86}Sr$ of lagoon waters and endmembers vs. salinity (PSU), note that the Lower Lake samples were too radiogenic to be plotted on the scale. (B) $\delta^{44/40}Ca$ of lagoon waters and endmembers vs. salinity (PSU).

- Normally, the North Lagoon is strongly controlled by seawater input from Southern Ocean; however, due to the amount of groundwater input, mixing between these two components are also significant.
- The South Lagoon is mostly hypersaline, as a result of seawater and radiogenic continental water/groundwater mixing and evaporation.
- As can be seen in Fig. 11A, $^{87}Sr/^{86}Sr$ signatures are efficient to recognise less radiogenic normal marine waters and radiogenic waters; however, the two radiogenic components (i.e. brackish and hypersaline waters) are impossible to be distinguished via Sr isotopes. The issue can be resolved by comparing $\delta^{44/40}Ca$ signatures, where the hypersaline waters have systematically positive $\delta^{44/40}Ca$ signatures up to ~ +0.2 ‰, and brackish and fresh waters yield negative $\delta^{44/40}Ca$ signatures, which can go to as low as ~ -0.77 ‰ (see Fig. 11B).
- $\delta^{44/40}Ca$ modelling estimated that 35-40% of of Ca in the waters of the South Lagoon were removed as carbonates as a result of the high evaporation rates (see 5.3.1.2).
- Otolith $^{87}Sr/^{86}Sr$ signatures can be considered as an integrated average values of local water signatures over the fish's lifetime where the data confirmed significant proportions of both seawater and groundwater input through the year; and Ca isotope data indicate that $\delta^{44/40}Ca$ in otoliths is primarily biologically controlled and might be used to quantify the rates of otoliths biomineralisation.
- Finally, this study in Coorong added potential to application of Sr and Ca isotopes on ancient environmental conditions, specifically paleo-salinity reconstructions based on $^{87}Sr/^{86}Sr$ and $\delta^{44/40}Ca$ in fossil archives.

ACKNOWLEDGMENTS

I acknowledge my supervisors Juraj Farkaš and Bronwyn Gillanders for directing the project, providing ideas, training on scientific works, organising the field trip and assisting with my thesis; David Bruce as our lab coordinator for training on TIMS and various lab working procedures; Chris Holmden for Ca isotope analyses at the Saskatchewan Isotope Laboratory in Canada; Christopher Izzo and Patrick Reis Santos for assistance in the field and providing ideas for my thesis; Jonathan Tyler and John Tibby for collaborating and providing useful ideas to the project; Aoife McFadden for training and analysing with solution ICP-MS at Adelaide Microscopy and Katie Howard for training on using epoxies, orgainising honours meetings and providing suggestions for our works. Nothing would have been done without these people.

The project was supported by the internal grant of University of Adelaide to Juraj Farkaš, and ARC support to Bronwyn Gillanders.

REFERENCES

BIRD, E. C. 1994. Physical setting and geomorphology of coastal lagoons. *Elsevier Oceanography Series,* **60**, 9-39.

BROWN, R. J., & SEVERIN, K. P. 2009. Otolith chemistry analyses indicate that water Sr: Ca is the primary factor influencing otolith Sr: Ca for freshwater and diadromous fish but not for marine fish. *Canadian Journal of Fisheries and Aquatic Sciences* **66**, 1790-1808.

CAPO, R. C., STEWART, B. W., & CHADWICK, O. A. 1998. Strontium isotopes as tracers of ecosystem processes: theory and methods. *Geoderma* **82**, 197-225.

CHESNEY, E. J., MCKEE, B. M., BLANCHARD, T., & CHAN, L. H. 1998. Chemistry of otoliths from juvenile menhaden Brevoortia patronus: evaluating strontium, strontium: calcium and strontium isotope ratios as environmental indicators. *Marine Ecology Progress Series*.

DORVAL, E., JONES, C. M., HANNIGAN, R., & MONTFRANS, J. V. 2007. Relating otolith chemistry to surface water chemistry in a coastal plain estuary. *Canadian Journal of Fisheries and Aquatic Sciences* **64**, 411-424.

DOUBLEDAY, Z. A., HARRIS, H. H., IZZO, C., & GILLANDERS, B. M. 2013. Strontium randomly substituting for calcium in fish otolith aragonite. *Analytical Chemistry* **86**, 865-869.

ELSDON, T. S., & GILLANDERS, B. M. 2002. Interactive effects of temperature and salinity on otolith chemistry: challenges for determining environmental histories of fish. *Canadian Journal of Fisheries and Aquatic Sciences* **59**, 1796-1808.

ELSDON, T. S., & GILLANDERS, B. M. 2003. Reconstructing migratory patterns of fish based on environmental influences on otolith chemistry. *Reviews in Fish Biology and Fisheries* **13**, 217-235.

ELSDON, T. S., & GILLANDERS, B. M. 2004. Fish otolith chemistry influenced by exposure to multiple environmental variables. *Journal of Experimental Marine Biology and Ecology* **313**, 269-284.

FANTLE, M. S., & TIPPER, E. T. 2014. Calcium isotopes in the global biogeochemical Ca cycle: Implications for development of a Ca isotope proxy. *Earth-Science Reviews* **129**, 148-177.

FARKAŠ, J., FRÝDA, J., & HOLMDEN, C. 2016. Calcium isotope constraints on the marine carbon cycle and CaCO 3 deposition during the late Silurian (Ludfordian) positive δ 13 C excursion. *Earth and Planetary Science Letters* **451**, 31-40.

FAURE, G. (1977). Principles of isotope geology.

FERNANDES, M., & TANNER, J. E. 2009. *Hypersalinity and phosphorus availability: the role of mineral precipitation in the Coorong lagoons of South Australia*: CSIRO Water for a Healthy Country.

FOWLER, A. J., CAMPANA, S. E., THORROLD, S. R., & JONES, C. M. 1995. Experimental assessment of the effect of temperature and salinity on elemental composition of otoliths using laser ablation ICPMS. *Canadian Journal of Fisheries and Aquatic Sciences* **52**, 1431-1441.

FRINGS, P. J., CLYMANS, W., FONTORBE, G., CHRISTINA, L., & CONLEY, D. J. 2016. The continental Si cycle and its impact on the ocean Si isotope budget. *Chemical Geology* **425**, 12-36.

GILLANDERS, B. M., & MUNRO, A. R. 2012. Hypersaline waters pose new challenges for reconstructing environmental histories of fish based on otolith chemistry. *Limnology and Oceanography* **57**, 1136.

GUSSONE, N., BÖHM, F., EISENHAUER, A., DIETZEL, M., HEUSER, A., TEICHERT, B. M., DULLO, W. C. 2005. Calcium isotope fractionation in calcite and aragonite. *Geochimica et cosmochimica acta* **69**, 4485-4494.

HAESE, R. R., GOW, L., WALLACE, L., & BRODIE, R. S. 2008. Identifying groundwater discharge in the Coorong (South Australia). *AUSGEO news* **91**, 1-6.

HAESE, R. R., WALLACE, L., & MURRAY, E. J. 2009. *Nutrient sources, water quality, and biogeochemical processes in the Coorong, South Australia*: Geoscience Australia.

HOFF, G. R., & FUIMAN, L. A. 1995. Environmentally induced variation in elemental composition of red drum (Sciaenops ocellatus) otoliths. *Bulletin of Marine Science* **56**, 578-591.

HOLMDEN, C., & BÉLANGER, N. 2010. Ca isotope cycling in a forested ecosystem. *Geochimica et cosmochimica acta* **74**, 995-1015.

KELL-DUIVESTEIN, I. 2015. *Tracing the groundwater inputs and water-mass mixing in the Coorong lagoons (South Australia) using strontium isotopes.* (Honours (Geology/Geophysics)), The University of Adelaide, Adelaide.

KJERFVE, B. 1986. Comparative oceanography of coastal lagoons. *Estuarine variability* **6381**.

KNOPPERS, B. 1994. Aquatic primary production in coastal lagoons. *Elsevier Oceanography Series* **60**, 243-286.

KRAUS, R. T., & SECOR, D. H. 2004. Incorporation of strontium into otoliths of an estuarine fish. *Journal of Experimental Marine Biology and Ecology* **302**, 85-106.

LAMBERTY, A., & PAUWELS, J. 1991. How to correct for blanks in isotope dilution mass spectrometry. *International Journal of Mass Spectrometry and Ion Processes* **104**, 45-48.

LUI, L. C. 1969. Salinity tolerance and osmoregulation of Taeniomembers microstomus (Gunther, 1861)(Pisces: Mugiliformes: Atherinidae) from Australian salt lakes. *Marine and Freshwater Research* **20**, 157-162.

MARTIN, G. B., & THORROLD, S. R. 2005. Temperature and salinity effects on magnesium, manganese, and barium incorporation in otoliths of larval and early juvenile spot Leiostomus xanthurus.

MARTIN, G. B., THORROLD, S. R., & JONES, C. M. 2004. Temperature and salinity effects on strontium incorporation in otoliths of larval spot (Leiostomus xanthurus). *Canadian Journal of Fisheries and Aquatic Sciences* **61**, 34-42.

MILTON, D. A., & CHENERY, S. R. 2001. Sources and uptake of trace metals in otoliths of juvenile barramundi (Lates calcarifer). *Journal of Experimental Marine Biology and Ecology* **264**, 47-65.

NÉGREL, P., & ROY, S. 1998. Chemistry of rainwater in the Massif Central (France): a strontium isotope and major element study. *Applied geochemistry* **13**, 941-952.

NOELL, C., & SCIENTIFIC, C. 2009. *Fish assemblages of the Murray Mouth and Coorong region, South Australia, during an extended drought period*: CSIRO Water for a Healthy Country National Research Flagship and South Australian Research and Development Institute (Aquatic Sciences).

NOYE, B. J. 1975. *The Coorong*: Department of Adult Education University of Adelaide.

ROLSTON, A., & DITTMANN, S. 2009. The Distribution and Abundance of Macrobenthic Invertebrates in the Murray Mouth and Coorong Lagoons 2006 to 2008. *Canberra, Australia CSIRO: Water for a Healthy Country National Research Flagship* **89**.

ROMANIELLO, S., FIELD, M., SMITH, H., GORDON, G., KIM, M., & ANBAR, A. D. 2015. Fully automated chromatographic purification of Sr and Ca for isotopic analysis. *Journal of Analytical Atomic Spectrometry* **30**, 1906-1912.

VON DER BORCH, C. C., LOCK, D. E., & SCHWEBEL, D. 1975. Ground-water formation of dolomite in the Coorong region of South Australia. *Geology* **3**, 283-285.

WALKER, D. J. 2003. Assessing environmental flow requirements for a river-dominated tidal inlet. *Journal of coastal research*, 171-179.

WEBSTER, I. T. 2010. The hydrodynamics and salinity regime of a coastal lagoon–The Coorong, Australia–Seasonal to multi-decadal timescales. *Estuarine, Coastal and Shelf Science* **90**, 264-274.

WEDDERBURN, S. D., BARNES, T. C., & HILLYARD, K. A. 2014. Shifts in fish assemblages indicate failed recovery of threatened species following prolonged drought in terminating lakes of the Murray–Darling Basin, Australia. *Hydrobiologia* **730**, 179-190.

APPENDIX A: DETAILS OF RESEARCH PTROTOCOLS

A.1. Chromatographic purification – modified sample purification method for Sr

Firstly, a total procedural blank of the element of interest (i.e., Sr) was determined via isotope dilution (for details see Appendix A.3.1), as it is desirable and important that the blank is less than 0.1% of the total amount of Sr loaded and originating from the sample. The volumes of water to be loaded was calculated based on Sr concentration results from solution ICP-MS, so that each sample contains about 1000 ng of Sr (see Table C2 in Appendix C), which is optimal as our typical procedural Sr blank on prepFAST-MC was about 0.1 ng (i.e., about 0.01% of total Sr from the sample).

For bulk Sr isotope analyses, one otolith per pair from each fish sample was analysed. The whole otolith was dissolved in 100 µL of 15M HNO_3 in a clean 7 mL round-bottomed PFA teflon vial, if the amount of Sr in the otolith was above 1000 ng (see Table C3 in Appendix C), only a half of the dissolved otolith solution was used. The otolith solution was then dried and re-dissolved with 1mL of 2M HNO_3. Micro-drilled otolith samples were directly dissolved with 1mL of 2M HNO_3 since these samples were in powder form.

All vials of samples in 2M HNO_3 solutions were labelled and transferred to the operation desk and autosampler unit of the prepFAST-MC system. The same number of clean 7 mL PFA vials were labelled and located in the rack to collect purified Sr from each sample.

The sample purification method for Sr was adapted from Romaniello et al. (2015). As listed in Table A1, 5 reagents were used in the method, but instead of 10 mL of Sr solution, only 6 mL were collected, and the remaining 4 mL were discarded since there was very little Sr left in the sample after 6 mL of acid elution, as tested by Romaniello et

al. (2015) on BCR-2 basalt, IAPSO seawater, CUE-0001 llama bone, and NIST-1400 bone ash. Therefore, 7 mL vials were used for collection instead of the 15 mL ones.

Table A1. Chromatographic steps for the automated separation of Sr by 1 mL ESI Sr–Ca column. Modified from Romaniello et al. (2015).

Step	Purpose	Volumn	Reagent
1	Condition column	10 mL	2 M HNO_3 + 1 wt% H_2O_2
2	Load sample	1 mL	2 M HNO_3
3	Elute sample matrix (not collected)	10 mL	2 M HNO_3 + 1 wt% H_2O_2
4	Elute Sr (collected)	6 mL	6M HNO_3
5	Elute Sr (not collected)	4 mL	6M HNO_3
6	Elute Ca (not collected)	10 mL	12 M HNO_3
7	Elute REEs, Hf, Cd, U and wash the column	10mL	1M HF

Once the method and purification procedure were finished, the column was stored in 2 M HNO_3 + 1 wt% H_2O_2. The Sr solutions collected with 6 mL vials were transferred onto a hotplate with the caps off to evaporate. A drop of 0.5M H_3PO_4 was added into each vial to prevent the purified Sr crystal from escaping. After the solutions were dried, the vials were recapped and transferred to the TIMS laboratory for isotope composition analysis.

A.2. TIMS analyses

For each sample, the loading process detailed below was followed. Solutions were dropped on parafilm before pipetting and loading.

Loading process:

Centre filaments with non-zone-refined Re ribbon was used, no inner or outer filaments were used.

1. Load 1 µL 1M H_3PO_4 and evaporate at 0.5-0.8 A.
2. Load 0.5 µL Bircks Solution and evaporate at 0.5 A.
3. Load ~500ng Sr in 1 µL Bircks Solution and dry st 0.5 A.
4. Gradually increase to ~1 A, but reduce current if load starts to spread.

5. Over about 1 minute, increase to 1.8 A and leave for 1 minute.
6. Heat to just red for several seconds, estimated at ~2.3-2.4 A.
7. Turn down the current and fix the filament onto the magazine, record sample names and details, corresponding to the position of the filaments.

Building of ion beams:

In the mass spectrometer, the ionisatoin (centre) filament current was ramped slowly to 2.3 A, about 30 minutes, then the current was turned up slowly to ~3.1-3.3 A, resulting in an ionisation temperature of ~1350-1400 ºC and a target ion beam intensity of ~5-6 A (^{88}Sr).

A.3. Data correction

A.3.1. PREPFAST-MC BLANKS AND TOTAL PROCEDURAL BLANKS (TPB)

To determine the contamination on Sr measurements introduced by prepFAST-MC, blanks were made and run at the beginning and the end of a sample sequence. An ^{84}Sr-enriched single spike with 81.60072% of ^{84}Sr and 3.47641% of ^{86}Sr and 13.38241% of ^{88}Sr was used in the procedure. To make a blank, 3 drops of single spike solution was added to a clean and labelled 7 mL round-bottomed PFA vial, and the mass of the spike was weighed and recorded. Then the spike solution was dried and dissolved with 1 mL of 2M HNO_3.

To determine the contamination caused by the acid dissolution process when preparing otoliths solutions for prepFAST-MC, total procedure blanks (TPB) were made and run together with the sample sequences. The making of TPB takes an extra step compared with normal prepFAST-MC blanks, which is adding 100 µL of 15M HNO_3 (i.e. the same

acid used to dissolve the otoliths) to the vial after the spike was weighed, and evaporate on the hotplate.

After purification by prepFAST-MC, the $^{84}Sr/^{88}Sr$ ratios of the solutions were measured by TIMS, and the amount of Sr in blanks were determined by Isotope Dilution, described by Lamberty and Pauwels (1991). The functions developed in Visual Basic modules and used in Microsoft Excel were:

```
Function Srblank(spike, wtsa, wtsp, Sr48)
'Using Faure p62, calculate blank Sr pg using spike D (db 22-3-2001).
'  Update of SrD()to measure 84/88Sr rather than 84/86Sr because of improved blanks (db 12-07-2015).

If spike = "A" Then
    uggSrsp = 1000000 * 0.0022949146 / 119.18786 'ugg-1 Sr spike A (19.05395398)
ElseIf spike = "B" Then
    uggSrsp = 1000000 * 0.0000298635 / 32.2311 'ugg-1 Sr spike B (.92654299729)
ElseIf spike = "C" Then
    uggSrsp = 1000000 * 5.51073 * 0.0022949146 / 119.18786 / 123.58436
    'ugg-1 Sr spike C (.858579)
ElseIf spike = "D" Then
    uggSrsp = 1000000 * 0.85529 * 5.51073 * 0.0022949146 / 119.18786 / 123.58436 / 112.23948
    'Sr spike D (6.77205ngg-1 Sr)db.
ElseIf spike = "F" Then
    uggSrsp = 1000000 * 0.85529 * 5.51073 * 0.0022949146 / 119.18786 / 123.58436 / 112.23948 * (10.38938 / 122.39867)
    'Sr spike F (.555342ngg-1 Sr)29/2/08db.
    Else: uggSrsp = "Error"
End If

ugSrsp = wtsp * uggSrsp 'ug Sr in the mixture contributed by the spike
wtSrsa = 87.62 'wt Sr sample (87.62 Chart of the nuclides 15th ed)
wtSrsp = 84.5718779 'wt Sr spike (84.5718779)
ab4Srsp = 0.8160072 'abundance 84Sr spike (from GEM's Sr unmixing program)?????
ab6Srsp = 0.0347641 'abundance 86Sr spike
ab8Srsp = 0.1338241 'abundance 88Sr spike (from GEM's Sr unmixing program)?????
ab4Srsa = 0.0056 'abundance 84Sr sample Chart of the nuclides 15th ed ?? and www.isotopx.co.uk
ab6Srsa = 0.0986 'abundance 86Sr sample Chart of the nuclides 15th ed ?? and www.isotopx.co.uk
ab8Srsa = 0.8258 'www.isotopx.co.uk

f2 = (ab4Srsp - Sr48 * ab8Srsp) / (Sr48 * ab8Srsa - ab4Srsa) 'factor 2
f1 = ugSrsp * wtSrsa / wtSrsp 'factor 1
f3 = f1 * f2 'wt Sr sample
Srblank = 1000000 * f3 / wtsa 'pgg-1 Sr sample

End Function
Function Cablank(WTSA, WTSPK, R4048MIX)
'Using Faure p62, calculate blank Sr pg using spike D (db 22-3-2001).
'  Update of SrD()to measure 84/88Sr rather than 84/86Sr because of improved blanks (db 12-07-2015).

R4048NATURAL = 96.941 / 0.187
R4048SPIKE = 0.02286919

CCaSPK = 10 ' ppm

Cablank = (R4048SPIKE - R4048MIX) / (R4048MIX - R4048NATURAL) * (1 + R4048NATURAL) / (1 + R4048SPK) * WTSPK / WTSA * CCaSPK 'ug

End Function
```

As a result, an average of ~100 pg Sr was detected per blank. We expect the blanks contain < 0.1 wt% of Sr as in the sample to be optimal, i.e. 100/0.1% = 100,000 pg = 100 ng Sr in sample. This is the preferred minimun amount of Sr per sample to be loaded on prepFAST-MC.

A.3.2. NIST SRM 987

NIST SRM 987 was used as a Sr standard for testing stability of TIMS, it is composed of pure strontium carbonate, and has well known published $^{87}Sr/^{86}Sr$ values. According to Georem, the value ranges from 0.701243 to 0.71395 based on 1416 data points, with a compiled value of 0.71034. 500 ng (200 µL) of NIST SRM 987 was loaded per filament. The average 2 standard error for $^{87}Sr/^{86}Sr$ data from TIMS is ±0.000003 (Table d).

A.3.3. INTERNATIONAL ASSOCIATION FOR THE PHYSICAL SCIENCES OF THE OCEAN (IAPSO) STANDARD SEAWATER

The IAPSO standard seawater is basically surface seawater collected from the Atlantic Ocean, and it was used to test the stability of prepFAST-MC. The published $^{87}Sr/^{86}Sr$ values from Georem range from 0.709134 to 0.70921 based on 9 data points. Although the $^{87}Sr/^{86}Sr$ value of IAPSO is not as well published as NIST SRM 987, the major advantage of using IAPSO for testing prepFAST-MC is that the chromatographic column's ability of separating elements can be well examinated as IAPSO contains all other elements in seawater instead of pure Sr. 125 µL (~1 µg Sr, ~50 µg Ca) of seawater was added into a clean 7 mL round-bottomed PFA vial for each standard and dried on a hotplate to white powder, then 1 mL of 2M HNO_3 was added to dissolve the powder. The solution was then run on prepFAST-MC with 6 mL of Sr solution being collected. The isotope compositions were then measured by TIMS. The average 2 standard error for $^{87}Sr/^{86}Sr$ through prepFAST-MC and TIMS is ±0.000006.

A.3.4. INTERNAL NORMALIZATION OF $^{87}SR/^{86}SR$

According to Capo et al. (1998), mass-dependent fractionation during measurements by the instruments was corrected by normalising to the $^{87}Sr/^{86}Sr$ ratio, which was set at 0.1194.

APPENDIX B: GEOLOGICAL HISTORY OF THE COORONG REGION

The formation of the world's coastlines was largely affected by the submerging of continental margins during the late Quaternary global marine transgression, which started about 18,000 years ago and was triggered by warming up of climate in an interglacial period (Bird, 1994). This directly resulted in the submergence of valley mouths to form inlets and estuaries throughout the world's coastlines due to sea level rise, including the Coorong. The lagoon was then enclosed and cut off from Encounter Bay by a series of calcareous sand barriers which were formed by uplifting over the last 6,000 years, forming a narrow-shaped water body over 110 km along the coastline (Bird, 1994; Webster, 2010).

APPENDIX C: SUPPLIMENTARY TABLES AND FIGURES

Table C1. Table of sampling locations and dates.

Sample ID[1]	Area	Position	Sampling Date	Latitude (degree South)	Longitude (degree East)
Coorong Lagoon water samples					
M13	Murray Mouth		April 28, 2016	35.55	138.88
C02	North Lagoon	Mark Point	May 16, 2016	35.62	139.08
C03	North Lagoon	Long Point	May 16, 2016	35.70	139.16
C04	North Lagoon	Noonameena	May 16, 2016	35.77	139.27
C05	North Lagoon	Rob's Point	May 16, 2016	35.79	139.32
C07	South Lagoon	Parnka Point North	May 16, 2016	35.89	139.40
C06	South Lagoon	Parnka Point	May 16, 2016	35.90	139.40
C08	South Lagoon	The end of Field Road	May 16, 2016	35.94	139.49
C09	South Lagoon	1.5 km south to the end of Woods Well Road	May 16, 2016	36.01	139.56
C10	South Lagoon	Policemen's Point	May 16, 2016	36.07	139.60
C11	South Lagoon	Salt Creek	May 16, 2016	36.13	139.64
C12	South Lagoon	1 km south to Pipe Clay Lake	May 16, 2016	36.16	139.65
SL9	South Lagoon	Site neat Halite Lake	April 10, 2015	36.16	139.65
SL8	South Lagoon	Pelet/Milne Lake (Ephemeral Lake)	April 10, 2015	36.14	139.65
SL7	South Lagoon	Policeman Point	April 10, 2015	36.06	139.59
SL6	South Lagoon	Woods Well	April 10, 2015	36.01	139.55
SL5C	South Lagoon	Seawater further from seepage site	April 10, 2015	35.96	139.50
SL5B	South Lagoon	Seawater close to seepage	April 10, 2015	35.95	139.50
SL4B	South Lagoon	Lagoon widest part	April 10, 2015	35.92	139.46
SL4A	South Lagoon	Lagoon widest part	April 10, 2015	35.91	139.46

SL1B	South Lagoon	Parnka Point	April 10, 2015	35.90	139.40
SL2	South Lagoon	Parnka Point	April 10, 2015	35.89	139.41
NL1	North Lagoon	Robs Point	April 10, 2015	35.80	139.32
NL2	North Lagoon	Near Robs Point	May 15, 2015	35.80	139.32
NL3	North Lagoon	North of Robs Point ~1.5km	May 15, 2015	35.79	139.31
NL4	North Lagoon	Near Emohruo	May 15, 2015	35.78	139.30
NL5	North Lagoon	North of NL4 ~1.5km	May 15, 2015	35.78	139.29
NL6	North Lagoon	Coorong Park	May 15, 2015	35.77	139.27
NL7	North Lagoon	Near Camp Aroonumeena	May 15, 2015	35.76	139.26
NLB1	North Lagoon	North Northern Lagoon, boat sample	May 15, 2015	35.70	139.16
NLB3	North Lagoon	North Northern Lagoon, boat sample	May 15, 2015	35.68	139.15
NLB4	North Lagoon	North Northern Lagoon, boat sample	May 15, 2015	35.68	139.14
NLB5	Northern Lagoon	North Northern Lagoon, boat sample	May 15, 2015	35.67	139.13
NLB6	North Lagoon	North Northern Lagoon, boat sample	May 15, 2015	35.66	139.12
NLB11	North Lagoon	North Northern Lagoon, boat sample	May 15, 2015	35.63	139.07
NLB15	North Lagoon	North Northern Lagoon, boat sample	May 15, 2015	35.59	139.02
Groundwater samples					
JWP2	North Lagoon (Groundwater)	Near Aroonumeena		35.79	139.31
BWP2	North Lagoon (Groundwater)	Near Aroonumeena		35.78	139.30
Lower Lakes, river and seawater samples					

C01	Lower Lakes connection	Narrung	May 16, 2016	35.51	139.19
LL1	Lake Albert	Pier in Meningie	May 15, 2015		
LL2	Lake Alexandrina		May 15, 2015	35.51	139.13
LL3	Lower Lakes Connection	Narrung	May 15, 2015	35.51	139.19
MR1	Murray River	Wellington ferry crossing	May 15, 2015	35.33	139.39
SL11	Southern Ocean	Open Ocean seawater	April 10, 2015	36.29	139.70
Rainwater samples					
Rain-IT (galvanized iron tank)	South Australia	10 km north to coastline	Sept. 13, 2016		
Rain-PT (polyethylene tank)	South Australia	10 km north to coastline	Sept. 13, 2016		
Rain-A Sr	South Australia	10 km north to coastline	Aug. 29-30, 2016		
Rain-B Sr	South Australia	10 km north to coastline	Aug. 29-30, 2016		

[1]refers to IDs of waterbody samples, fish/otoliths samples collected at the same location are labelled as "waterbody sample ID-XX", where XX is the code for the fish.

Table C2. List of volumes of water samples being used for prepFAST-MC purification in 2016. The Sr concentration of rainwater samples were estimated to be ~ 0.02 µmol/L according to Négrel and Roy (1998).

Sample ID	Volume of sample per 1ug Sr (uL)	Sampling Year
C01	1500	2016
C02	125	2016
C03	140	2016
C04	125	2016
C05	125	2016
C06	70	2016
C07	88	2016
C08	40	2016
C09	70	2016
C10	50	2016
C11	48	2016
C12	40	2016
M14	125	2016
SL4B	53	2015
SL5B	53	2015
SL5C	49	2015
SL6	54	2015
SL7	41	2015
SL8	16	2015
SL9	37	2015
SL10	20	2015
NL1	123	2015
NL2	212	2015
NL3	210	2015
NL4	224	2015
NL5	232	2015
NLB4	153	2015
NLB5	141	2015
Rain-IT (galvanized iron tank)	500,000	2016
Rain-PT (polyethylene tank)	500,000	2016
Rain-A Sr	500,000	2016
Rain-B Sr	500,000	2016

Table C3. Table of fish sample parameters. Minimum Sr content in otoliths samples, calculated based on otoliths weights and the minimum concentration of Sr, which is about 1000 ppm (Doubleday, Harris, Izzo, & Gillanders, 2013).

Sample ID	Fish body length (mm)	Fish weight (g)	Single otolith weight (mg)	Minimum Sr in a single otolith (ng)
M13-01	51	0.74	0.954	954
M13-02	56	1.02	1.162	1162

M13-14	61	1.53	1.317	1317
C03-02	54	1.10	1.169	1169
C03-03	69	2.52	1.495	1495
C03-04	54	1.28	1.300	1300
C03-05	55	1.18	1.197	1197
C04-01	50	0.79	0.831	831
C04-02	41	0.49	0.595	595
C04-03	47	0.73	0.865	865
C07-01	35	0.27	0.481	481
C07-02	41	0.41	0.586	586
C06-02	36	0.42	0.682	682
C06-04	40	0.40	0.634	634
C08-01	41	0.45	0.602	602
C08-03	36	0.28	0.513	513
C09-01	43	0.53	0.750	750
C09-02	36	0.33	0.515	515
C10-01	55	1.39	1.277	1277
C10-03	68	2.13	2.139	2139
C10-05	48	0.90	1.048	1048
C11-01	39	0.43	0.614	614
C11-03	34	0.36	0.633	633
C12-01	30	0.19	0.300	300
C12-02	29	0.15	0.305	305
C12-03	28	0.15	0.301	301

Table C4. Elemental concentrations (in ppm) of waterbody samples and standard seawater (OSIL) measured by solution ICP-MS.

Sample name	Salinity (PSU)	Na	Mg	Al	Ca	Ti	Cr	Mn	Fe	Cu	Zn	Sr	Ba
LL2	0.43	125.9	21.1	0.0020	35.2	0.45	0.00024	0.00026	0.009	0.0105	0.0027	0.32	0.0558
C01	0.80	181.2	29.9	0.0045	33.1	0.63	0.00047	0.00068	0.014	0.0061	0.0136	0.48	0.0752
LL1	1.29	369.5	58.6	0.0042	46.5	0.61	0.00027	0.00031	0.019	0.0277	0.0051	0.88	0.0980
NL3	19.50	5582.5	676.4	0.0101	213.3	1.76	0.00087	0.00034	0.047	0.0031	0.0031	4.56	0.0197
NL2	19.69	7721.3	946.8	0.0119	301.0	6.89	0.00189	0.00185	0.059	0.0076	0.0038	6.05	0.0172
NL4	20.09	5552.4	681.2	0.0140	201.9	5.29	0.00124	0.00069	0.048	0.0027	0.0044	4.51	0.0195
NL5	20.75	6034.8	732.6	0.0131	205.9	7.90	0.00280	0.00060	0.056	0.0026	0.0112	4.80	0.0206
NLB4	29.53	9120.4	1117.9	0.0028	313.9	0.96	0.00200	0.00162	0.062	0.0059	0	7.18	0.0165
NLB5	32.19	9760.4	1192.0	0	402.4	1.75	0.00148	0.00163	0.065	0.0049	0	7.74	0.0127
C03	32.96	9448.5	1162.3	0	336.5	7.21	0.00212	0.00123	0.067	0.0028	0.0068	7.56	0.0086
C05	34.05	9945.7	1216.6	0	382.5	1.23	0.00130	0.00560	0.067	0.0015	0	8.42	0.0113
NL1	34.44	10715.9	1298.4	0.0265	355.9	8.28	0.00165	0.00049	0.074	0.0026	0.0043	8.86	0.0213
C04	34.67	10129.6	1247.9	0.0009	367.2	4.39	0.00176	0.00355	0.073	0.0024	0.0376	8.10	0.0095
OSIL	35.00	11333.6	1374.6	0.0098	390.4	2.09	0.02781	0.00177	0.181	0.0023	0.0462	8.86	0.0028
C02	34.98	10377.8	1275.1	0.0213	382.9	8.75	0.00567	0.00726	0.084	0.0035	0.0576	8.16	0.0083
C07	56.97	12821.8	1567.9	0.0025	445.8	2.37	0.00206	0.00053	0.084	0.0021	0	10.57	0.0194
C06	63.73	19981.0	2409.1	0.0150	652.3	3.17	0.00268	0.00255	0.131	0.0027	0	16.15	0.0268
C09	65.45	19792.3	2407.1	0.0011	638.6	3.22	0.00256	0.00353	0.128	0.0035	0.0067	15.87	0.0265
SL5B	81.55	24432.5	2936.4	0	780.5	2.74	0.00238	0.00104	0.160	0.0049	0	19.95	0.0255
SL5C	82.10	24479.1	2905.5	0.0092	798.1	4.27	0.00245	0.00127	0.169	0.0051	0.0006	20.16	0.0264
SL4B	83.30	25223.6	3067.7	0	795.6	3.80	0.00233	0.00095	0.166	0.0062	0	20.78	0.0252
C10	84.10	25442.0	3026.6	0.0027	814.4	6.10	0.00399	0.00837	0.183	0.0075	0.0023	19.87	0.0294
C11	85.10	25689.7	3106.6	0.0217	802.7	3.26	0.00440	0.01049	0.170	0.0072	0.0414	19.95	0.0298
SL6	89.35	29316.3	3537.0	0.0130	883.5	3.69	0.00297	0.00081	0.196	0.0058	0.0013	23.56	0.0272

C08	93.40	13428.0	1653.0	0.0064	433.5	6.53	0.00361	0.01886	0.176	0.0054	0.0023	11.16	0.0304
C12	94.10	26618.3	3204.0	0.0038	810.5	5.85	0.00577	0.00484	0.174	0.0044	0	20.65	0.0290
SL7	104.65	32761.2	3962.2	0.0231	986.1	6.09	0.00305	0.00336	0.205	0.0083	0.0031	25.51	0.0275
SL8	108.10	36897.0	2698.3	0.0052	69.1	5.13	0.00516	0.00036	0.033	0.0086	0.0005	58.11	0.0479
SL9	113.60	37147.4	4373.1	0.0259	1066.3	13.62	0.00318	0.00136	0.235	0.0111	0.0053	28.09	0.0300
SL10	137.30	46293.9	5284.7	0.0895	656.3	9.86	0.00436	0.00134	0.149	0.0147	0.0084	55.33	0.0484

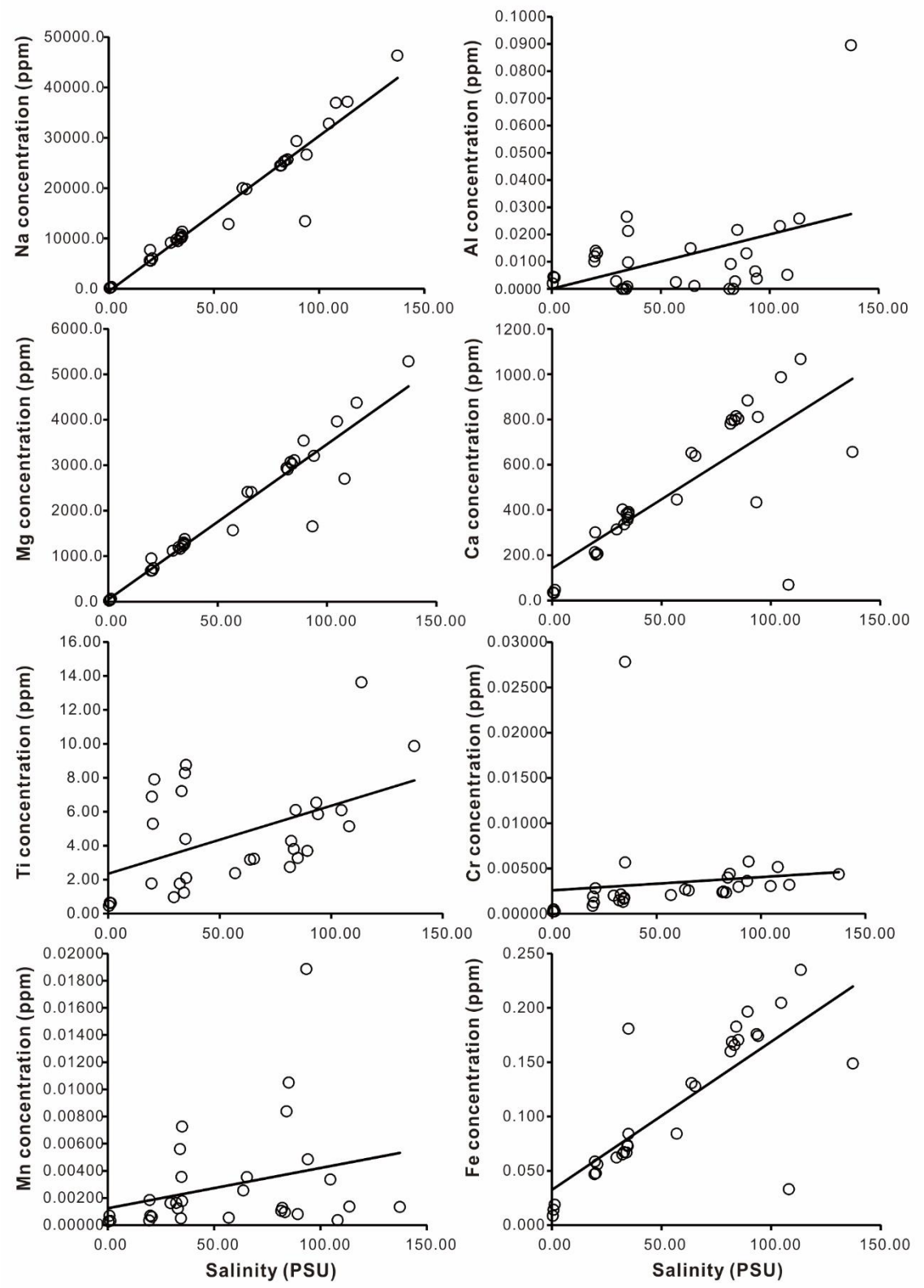
Na concentration (ppm)
Al concentration (ppm)
Mg concentration (ppm)
Ca concentration (ppm)
Ti concentration (ppm)
Cr concentration (ppm)
Mn concentration (ppm)
Fe concentration (ppm)
Salinity (PSU)
Salinity (PSU)

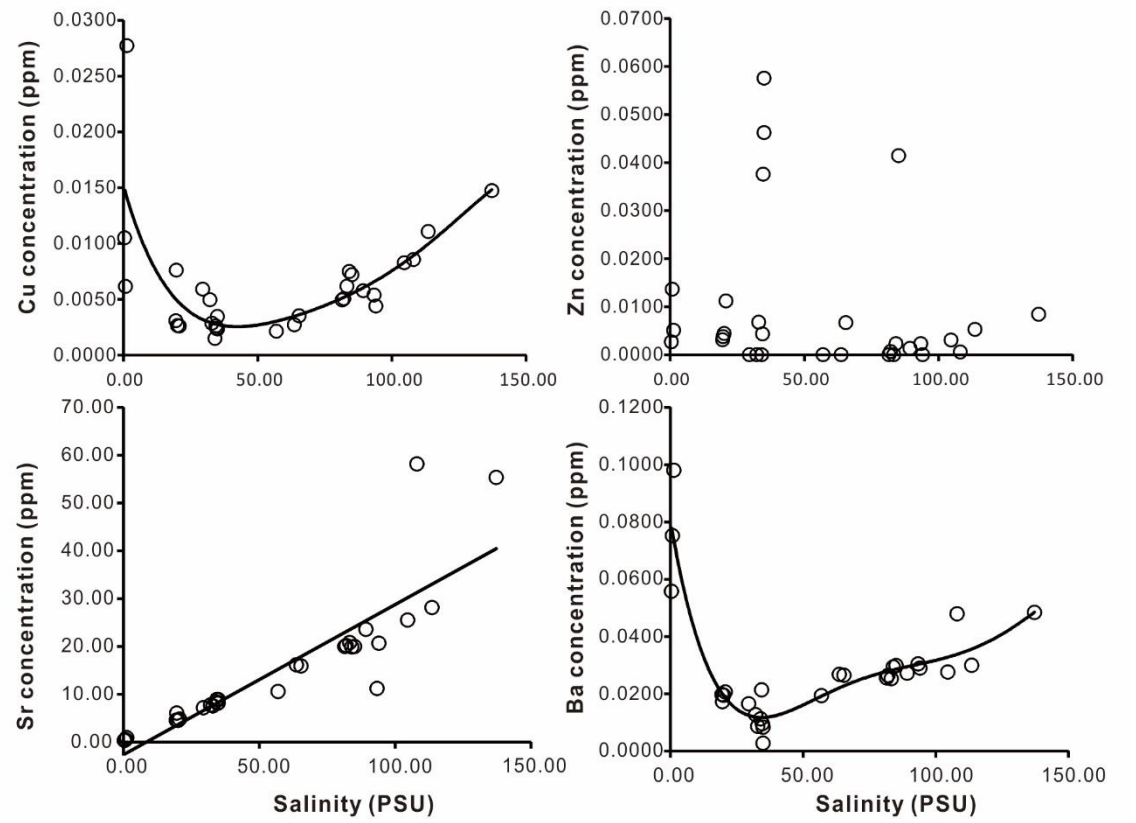

Figure C1: Elemental concentrations (ppm) vs. salinity (PSU) for waterbody samples collected in May 2016.

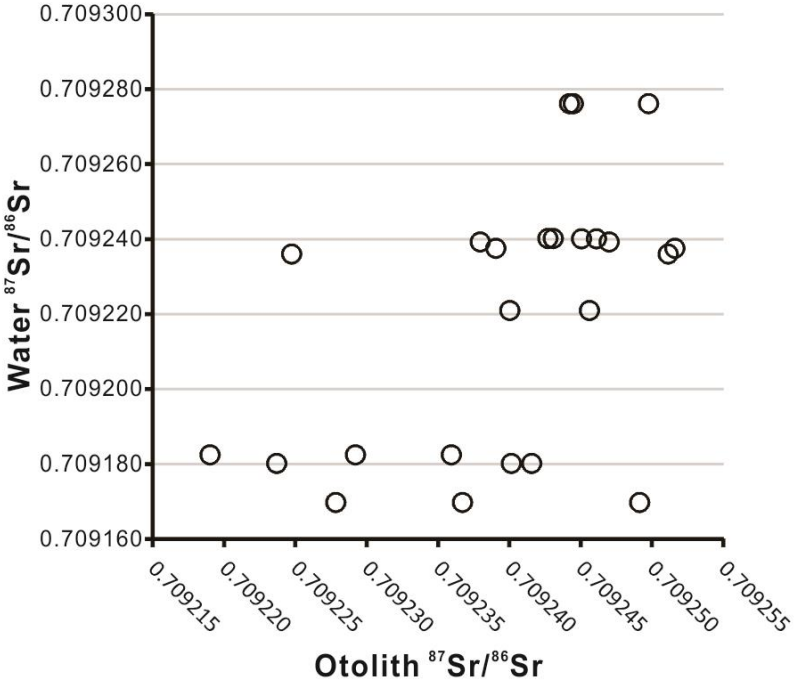

Figure C2: $^{87}Sr/^{86}Sr$ in 2016 Coorong Lagoon water samples vs. $^{87}Sr/^{86}Sr$ in fish otolith.

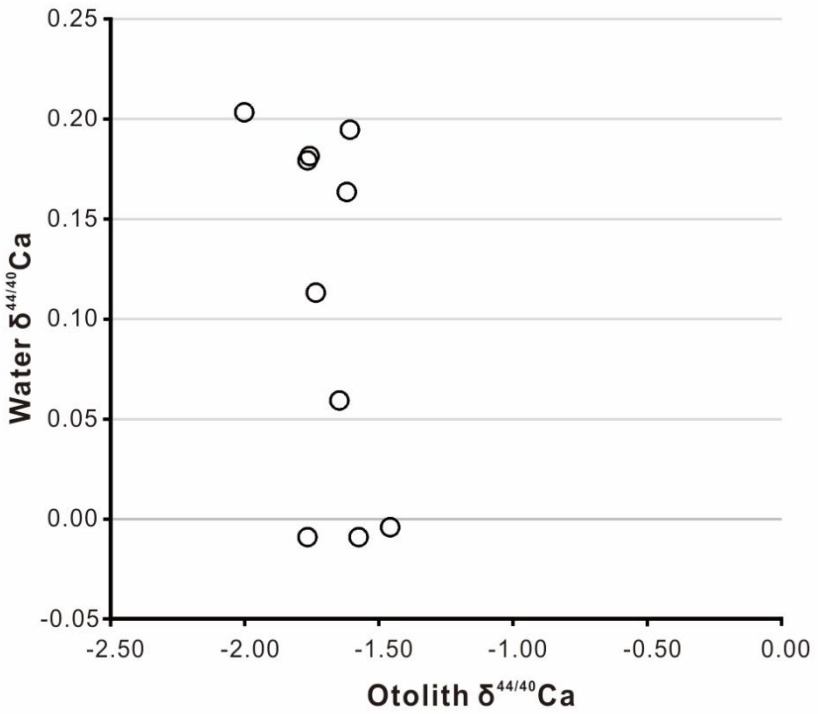

Figure C3: $\delta^{44/40}$Ca in 2016 Coorong Lagoon water samples vs. $\delta^{44/40}$Ca in fish otolith.